Energy, Mines and Resources Canada | Énergie, Mines et Ressources Canada

CANMET

Canada Centre for Mineral and Energy Technology | Centre canadien de la technologie des minéraux et de l'énergie

INTERFACIAL PHENOMENA IN COAL TECHNOLOGY
PART I. SURFACE CHARACTERIZATION OF COAL

E.I. Vargha-Butler, D.R. Absolom, H.A. Hamza and A.W. Neumann

January 1986

The format of this report is of that indicated by publisher

This document is an interim report prepared by the Coal Research Laboratories, Energy Research Program, CANMET

Ce document est un rapport provisoire préparé par les Laboratoires de recherche sur le charbon, Programme de l'énergie, CANMET

Cette version définitive de l'opinion du Centre canadien de la technologie des minéraux et de l'énergie (CANMET)

88 pp

ENERGY RESEARCH PROGRAM
COAL RESEARCH LABORATORIES
P.O. BAG 1280
DEVON, ALBERTA
ERP/CRL 86-6(TR)

MICROMEDIA
MAY 03 1988

G.D. Botsaris and

Y.M. Glazman

"Interfacial Phenomena In Coal Technology"

Part I. Surface Characterization of Coal

Chapter 2 "Characterization of Coal by Contact Angle and Surface Tension Measurements"

Authors: E.I. Vargha-Butler,[1], D.R. Absolom,[1]
H.A. Hamza[2] and A.W. Neumann[1]

[1]Department of Mechanical Engineering
University of Toronto
5 King's College, Road
Toronto, Ontario, M5S 1A4
Canada

[2]EMR, CANMET
Devon Coal Research Center
1 Oil Patch Drive
Devon, Alberta, TOC 1E0
Canada

CHAPTER TABLE OF CONTENTS

I. INTRODUCTION

II. THEORETICAL ASPECTS OF SURFACE TENSION

III. EXPERIMENTAL TECHNIQUES

3.1. Direct Contact Angle Measurements

3.2. Indirect Techniques

3.2.1. Advancing Solidification Front

3.2.2. Sedimentation Volume

3.2.3. Particle Adhesion

IV. DISCUSSION

4.1. Comparison of the Results Obtained by Different Techniques

4.2. Applicability and Range of Validity of the Different Techniques

V. APPENDIX

5.1. List of Symbols

5.2. Characterization of Coal Samples Discussed

VI. REFERENCES

I. INTRODUCTION

It has long been recognized that the characterization of the surface properties of coal can provide information relevant to coal processing, e.g. flotation. The main properties that are likely to be involved are surface tension and its manifestations, such as contact angles, and surface charge density.

In view of the importance of these properties a large number of investigators have concentrated their efforts on examining these problems. We propose not to review those efforts here. Instead the interested reader is referred to the comprehensive review articles on this subject [1]. An extensive bibliography of such work is available from the authors on request. In this article we propose to focus on more recent investigations related to the development of various techniques for the surface characterization of small particles in general and the application to coal fines. The various methods available for measuring surface charge have been extensively reviewed elsewhere [2].

The measurement of wettability of small particles is a difficult problem generally and is even more difficult in the case of coal. This is due, in part, to the heterogeneity in chemical composition, particle size and irregularity of particle shape. In spite of these problems several techniques are now available which are capable of yielding quantitative information on the wettability and surface tension of coal fines.

Before discussing the various experimental strategies we consider some fundamentals related to the concept of surface tension.

II. THEORETICAL ASPECTS OF SURFACE TENSION

In analogy with bulk phases, various thermodynamic properties can be defined for a surface. For example, the surface energy, $U^{(A)}$ of a flat surface can be defined as [3,4]

$$U^{(A)} = U^{(A)} (S^{(A)}, A, N_i^{(A)}) \qquad (1)$$

where $S^{(A)}$ is the surface entropy, A is the surface area, $N_i^{(A)}$ is the number of moles of component i in the surface. The surface tension, γ is then defined as:

$$\gamma = \left(\frac{\partial U^{(A)}}{\partial A}\right)_{S^{(A)}, N_i^{(A)}} \qquad (2)$$

The surface tension can, of course, be defined instead in terms of derivatives of the Legendre transforms of the surface energy [5]. The surface need not consist of one component but can consist of several components. If these components are uniformly distributed, the surface can be considered homogeneous, with a surface tension as defined above. Complications may arise when the surface of a multi-component system consists of patches of different composition. Nevertheless, if these patches are below a critical size, of the order of 0.1 μm [6], the surface can be considered homogeneous with respect to wetting phenomena. If the patches are above this critical size, the surface is heterogeneous, with different surface tensions as defined above for each patch.

The concept of surface tension as introduced above assumes that the phase under consideration is bounded by a vacuum. In cases where the phase under consideration borders on a second phase, the surface tension for that interface, i.e. the interfacial tension, is determined by the nature of both phases. For example, for a solid-liquid interface the value of the interfacial tension, γ_{SL}, will depend on which solid and liquid are present. Since the value

of the interfacial tension of, e.g., a solid depends on the phase with which the solid is in contact, some reference state must be chosen which reflects the surface properties of the solid alone. That reference state is chosen as the solid in contact with its own vapour. Thus, the surface tension of a solid, γ_S, is defined as the surface tension for the interface between the solid and its vapour. This surface tension cannot be measured directly; it can however be related to the interfacial tension γ_{SV}, between the solid and the vapour of some other material such as a liquid. When the solid surface is brought into contact with such a vapour, some of the vapour may be adsorbed onto the solid surface, lowering the surface tension of that solid. The difference between γ_S and γ_{SV} is called the equilibrium spreading pressure. Very often, particularly for "low energy" surfaces, e.g. Teflon, the adsorption of the vapour is negligible and the spreading pressure is small. The surface tension for the interface between the solid and the vapour, γ_{SV}, is then essentially the same as the solid surface tension, γ_S. Therefore, the value of the solid surface tension is often taken to be the value of γ_{SV}.

The determination of surface tensions of solids is possible only by indirect means and hence is inherently complex. Until a few years ago the only genearal approach to determine surface tensions of solids utilized contact angle measurements. To that end, an empirical equation of state approach for determining interfacial tensions has been developed [7-9]. In essense, this approach establishes that if a liquid (L) is in contact with a solid (S), then the interfacial tension γ_{SL} between the solid and liquid is given by an equation of state type of relation

$$\gamma_{SL} = f(\gamma_{SV}, \gamma_{LV}) \qquad (3)$$

Here γ_{SV} and γ_{LV} are the solid and liquid surface tensions, respectively. Equation (3) when formulated explicitly, can be used in conjunction with Young's equation

$$\gamma_{SV} - \gamma_{SL} = \gamma_{LV} \cos \theta \qquad (4)$$

where θ is the contact angle between the solid and a drop of liquid, to determine γ_{SV} and γ_{SL} from γ_{LV} and θ only. The latter two quantities are, in principle, readily obtained from direct experimental measurement, provided that a smooth and homogeneous solid surface of adequate size is available.

Using experimental contact angle data and liquid-vapour interfacial tensions, Eq. (3) has been formulated explicitly [7] as follows:

$$\gamma_{SL} = \frac{(\sqrt{\gamma_{SV}} - \sqrt{\gamma_{LV}})^2}{1-0.015\sqrt{\gamma_{SV}\cdot\gamma_{LV}}} \qquad (5)$$

In conjunction with Youngs Equation (4) the following relationship can be established:

$$\cos\theta = \frac{(0.015\,\gamma_{SV} - 2.00)\,(\sqrt{\gamma_{SV}\cdot\gamma_{LV}} + \gamma_{LV})}{\gamma_{LV}(0.015\sqrt{\gamma_{SV}\cdot\gamma_{LV}} - 1)} \qquad (6)$$

Equations (5) and (6) have, as they stand, certain purely mathematical limitations which can, however, be circumvented [7]. Computer programs [7,10] as well as Tables [11] which allow the determination of γ_{SV} and γ_{SL} for a wide range of γ_{LV} and θ values are available. It also should be remembered that for the approximation $\gamma_S \approx \gamma_{SV}$ to hold, i.e. for equilibrium spreading pressures to be negligible, the surface tension of the measuring liquid must be larger than the surface tension of the material on which the contact angle is determined.

III. EXPERIMENTAL TECHNIQUES

3.1. Direct Contact Angle Measurements

Historically this was the earliest method to be employed for measuring the wettability of coal [12,13]. Numerous papers have been published reporting the measurement of contact angles on coal surfaces. Whilst it is without question possible to obtain contact angle values for coal one must question what those measurements actually mean. In view of the widespread use of this technique we should like to discuss the basis of contact angle measurements in general as well as the associated pitfalls relative to coal.

Numerous techniques are available for the measurement of contact angles on flat surfaces. These techniques were reviewed recently [14]. Contact angle measurements have generally been performed on coal segments either cut from bulk coal samples [12,13,15,16] or on compressed tablets formed from coal particles [17,18]. Several criteria have been established empirically for the selection of samples for contact angle measurements [13,15,19,21-26]. Those criteria are listed in Table 1. However, it is that very selection process which gives rise to concern as to what the experimental data actually mean. Some of these conventional criteria, e.g. crack-free specimens, are sensible but others, such as the recommendation that only samples from "the jet black bands of bright coal" [13] should be used, are questionable. Coal is a markedly heterogeneous material and its overall composition will reflect its behaviour and must be taken into account. Contact angle measurements on preselected samples or areas of a coal specimen will likely give rise to biased data.

The other point which should be raised is the well established practice of polishing coal samples [15,22,24,25,26]. This has the advantage that it gives rise to smooth surfaces suitable for contact angle measurements. Unfortunately, however, the methodology has the disadvantage that in essence it gives rise to "new" coal surfaces which may differ markedly from those of the natural coal [15,27].

Various strategies are available for polishing coal [24-26]. One such method is described below.

Small segments of coal are produced with the use of a low speed circular saw. The coal surface is cooled during the cutting process with tap water to minimize any alteration due to the generation of heat.

The surface of the cut segment is then wet-ground using tap water with silicon carbide papers. Different grades of grit papers can be used to effect different polishes. In order to produce a fine finish, the medium-ground surfaces are further wet-polished with either napped Nylon or Microcloth. Standard polishing suspensions should not be used since the addition of a chemical lubricating compound would contaminate the coal surface rendering subsequent contact angle measurements meaningless.

After fine-polishing, the coal segments are rinsed with deionized distilled water and then stored in an evacuated desiccator in which anhydrous copper sulphate had been placed to remove any water. The storage desiccator is kept evacuated to prevent subsequent contamination of the coal surfaces prior to measurements.

Having thus prepared the coal surface it is then possible to measure contact angles on that surface.

The contact angle, θ, of a liquid on a solid surface is defined by the mechanical equilibrium of the drop under the action of three interfacial tensions, as discussed in connection with Young's Equation (4).

This equation is based on the assumption of ideal conditions and, as a result, it yields a single unique contact angle value. For almost any real surface, including coal, contact angle hysteresis is observed, i.e. the contact angle made by the advancing liquid droplet (θ_A) and that made by a receding liquid droplet (θ_R) are not equal. Contact angle hysteresis has been discussed in detail elsewhere [28]. Suffice it to say here that on a smooth surface the advancing contact angle value is a measure of the surface tension of the low energy sites on the coal surface, whilst the receding value is a measure of the high energy sites. Roughness is a second cause of contact angle hysteresis.

Several methods are available for measuring contact angles on flat surfaces [14] such as the tilting plate, capillary rise at a vertical plate [14], captive bubble [12,13,22] and sessile drop techniques [14,19,22]. Of these the sessile drop method is the most convenient to use with coal surfaces. It has two significant advantages: it requires only small quantities of measuring liquid, and coal samples with surfaces as small as a few square millimeters can be used.

The equipment required for such measurements are a horizontal levelled surface on which to place the coal surface, a micropipette with which to deposit a liquid drop onto the material and a means to observe the contact of the liquid with the surface of the material of interest. The delivery pipette should at all times remain in contact with the drop during the measurement process. This allows fluid to be added slowly to the drop, thereby creating a slowly advanc-

ing three phase line. For convenience, the size of the liquid droplets is chosen in the range of 2 - 4 mm. The contact angle which the liquid makes with the coal surface is then determined. In all cases both sides of the droplet should be measured in order to check the symmetry of the drop. If the drop is not symmetrical the observed readings should be disregarded. The volume of the drop is then slowly increased by adding more liquid and the contact angles on both sides of the drop again determined. Several techniques are available for actually measuring this contact angle [14]; a telescope with a goniometer eyepiece is the most convenient experimental set-up, its only drawback being limited accuracy. But for contact angle measurements on coal, accuracy will not normally be the issue, in view of the many complexities involved. If needed, significantly higher accuracy can be obtained by Axisymmetric Drop Shape Analysis (ADSA) [29,30]. In this approach photographs of sessile drops are obtained and the drop profile is digitized, and fitted to a numerical solution of the Laplace equation of capillarity, with the surface tension and the contact angle as adjustable parameters.

Using any of these techniques, it is thus possible to measure contact angles on polished coal surfaces. Nevertheless, the question still remains as to what these measurements actually mean. As an illustration of potential problems we wish to consider the following: it is well known that surface tensions, γ_{SV}, of homogeneous solids can be calculated via the equation of state approach [7] from the contact angles which liquids make on well prepared smooth, low energy surfaces. The surface tensions of these materials obtained in this manner are independent of the liquid used to measure such angles as is illustrated in Table 2 for a smooth Teflon surface. If a small segment of this surface is now "polished" under conditions similar to those used for coal

segments, as described above, and the contact angles again measured the contact angle results are different, as shown in Table 2. These data also show that the γ_{SV} values differ from one liquid to the next, and are therefore essentially meaningless. These observations give rise to concern about the significance of contact angle measurements on polished coal fragments.

As there are, at the moment, no general criteria to answer the question of how smooth is "smooth", one has to take recourse to schemes such as that implied for the smooth Teflon surface in Table 2, i.e. one may want to accept contact angle data as being correct (in the sense of being thermodynamically significant) if they predict the same γ_{SV} values virtually independently of the measuring liquids used.

As an illustration the advancing contact angles of water, glycerol and ethylene glycol on three different bituminous Canadian coal samples with five different surface finishes are given in Table 3 [24,25]. The results indicate that the contact angle for any of the liquids may or may not change considerably with polish, with no clear trends. Surprisingly, contact angles measured with water show that θ does not change in any regular manner with decreasing surface roughness. However, by using organic liquids rather than water for these measurements, the contact angles tend to increase with increasing coal surface smoothness. Coal surface tension values, γ_{SV}, calculated from these contact angle data <u>via</u> the equation of state approach [7] are given in Table 4. The point to be made with respect to these data is that it is quite clear that even on the Microcloth polished "smooth" coal surfaces different measuring liquids give rise to values of the surface tension which differ considerably. This observation brings into question the thermodynamic status of the contact angle measured on these surfaces. Comparing the effect of

surface roughness of the chemically homogeneous Teflon and of the heterogeneous coal samples (Tables 2 and 3), it is apparent that the observed contact angles decrease with decreasing roughness for Teflon, but for coal the reverse situation is observed. This situation is not yet fully understood but must be related to the heterogeneity of coal.

Thus on the basis of these results, it must be concluded that the direct contact angle measurement technique should be viewed as having only a limited scope for determining the intrinsic wettability of coal surfaces.

In addition to these concerns, it must also be realized that the polished coal surface, even if it allows the determination of a thermodynamically meaningful contact angle, may have little in common with the natural coal surface. If such measurements are to be performed at all it is, as a minimum requirement, desirable to perform tests with different liquids, and test for constancy of γ_{SV}, as in Table 2 and 4.

These comments are not necessarily meant to discourage the use of direct contact angle measurements on polished sections of coal. Such measurements probably contain a great deal of information, which, for the time being, we do not understand well. In this situation, additional techniques, such as those described in the remainder of this article, may be helpful. A point in question is the contact angle results for the "Coal Valley" sample of Tables 3 and 4. From solidification front measurements, see Table 6 below, we know that the surface tension of this coal is approximately 40 mJ/m^2. This is in reasonable agreement with the contact angle results obtained with ethylene glycol and glycerol, but at variance with the value obtained from the contact angle measurement with water. These facts probably make the latter data suspect. Indeed, a microscopic investigation of the Coal Valley specimens

revealed substantial amounts of inclusions of clay, and it appears likely that the contact with the sessile water drop caused swelling of the clay and capillary penetration processes, which affected the macroscopic contact angle. If this reasoning is correct, then the contact angle measurement with water would have to be rejected as a means of determining the surface tension of this particular coal sample. It is one of the purposes of the remainder of this article to put the investigator in a position where he can do better than giving a naive interpretation of directly observed contact angles.

3.2. Indirect Techniques

In recent years, we have developed several strategies to determine the surface tension of small particles; we have used these techniques, inter alia, to determine surface tension and contact angles of coal fines. These techniques are the advancing solidification front technique [31-35], sedimentation volume studies [36] and the particle adhesion method [37,38]. The relative merits and optimum conditions for each of these techniques will be discussed later in this article (cf. Section 4).

In each of these techniques, particle surface tensions are derived from thermodynamic models involving the relevant surface and interfacial tensions for the processes involved. As a matter of course solid-liquid interfacial tensions in these models have been written in terms of the equation of state for interfacial tensions [7] described earlier (cf. Section 2). The validity of the use of the equation of state approach in interpreting the data in each of these techniques has been discussed in detail elsewhere [39]. Here we only note that none of the methods described below a priori require the use of the equation of state approach. Identical results are obtained if other equations (e.g. Antonow's Rule) are used as equation of state.

3.2.1. Advancing Solidification Front

Historically [40], this method evolved in the mid-1970's as a means of testing various contact angle based approaches for determining surface tensions. This work revealed that both the associated thermodynamic model (described below) and the equation of state approach were valid. The method was subsequently developed into an analytical tool for determining the surface tension, γ_{PV}, of small particles [31,35].

The interaction of small particles with solidification fronts is a phenomenon of interest from several points of view. A particle, initially suspended in a liquid, will encounter a solid-liquid interface upon solidification of the liquid. At relatively low rates of solidification, the particle may either be engulfed by the advancing solidification front or else be swept along with it.

At low rates of solidification and in the absence of electrostatic interactions, inert particles may be expected to be engulfed, as illustrated schematically in Fig. 1, if the net change in the free energy of engulfment is negative

$$\Delta F^{eng} = \gamma_{PS} - \gamma_{PL} \qquad (7)$$

where γ_{PS} is the particle-solid interfacial tension and γ_{PL} is the particle-liquid interfacial tension. If ΔF^{eng} is positive, rejection and pushing of the particle by the advancing solidification front is to be expected. Which of these two processes will occur is dependent on the surface tension, γ_{PV}, of the particle.

However, in practice it is the free energy of adhesion (ΔF^{adh})

$$\Delta F^{adh} = \gamma_{PS} - \gamma_{PL} - \gamma_{SL} \qquad (8)$$

which is operative rather than ΔF^{eng} since once the particle is attached to the advancing solidification front it will be held there mechanically and

further solidification of the melt will keep the particle in its initial position, which will now be inside the solid phase, even if ΔF^{eng} is positive. The respective roles of ΔF^{eng} and ΔF^{adh} have been discussed in detail elsewhere [34]. In any case, the solid-liquid interfacial tension between solid and liquid matrix material is small for most materials, so that ΔF^{eng} and ΔF^{adh} carry the same sign.

Particle interaction with the solidification front is studied in a cell constructed from a copper block (80 mm x 30 mm x 5 mm) with a machined groove (30 mm x 5 mm x 0.6 mm) in the direction of the largest dimension. In order to establish a temperature gradient along the groove, the cell is heated electrically at one end while the other end is cooled by water circulating through the copper cooling coil. Constant rate of solidification can be effected with the temperature programmer by means of which the thermostat water can be heated and cooled at constant rates. The velocity of the advancing front can be changed over a wide range, from approximately 1 μm/sec to 100 μm/sec. A schematic of the apparatus is shown in Fig. 2.

For the engulfing experiments, the copper chamber is first washed with deionized distilled water and then rinsed with methanol, acetone and benzene. Particles are placed in the groove and covered with powdered matrix material. The chamber is then covered with a #2 glass coverslip (24 x 60 mm) which had previously been washed with distilled water, methanol, acetone and benzene. The purpose of the coverslip is to protect the melt from the effects of the local environment, e.g. ambient temperature, air currents, etc.

The solidification front-particle interaction may be observed through the microscope using reflected light, a suitable long-working distance objective lens and appropriate polarizing filters. Typical photomicrographs are given

in Fig. 3. Attached to the microscope is a videocamera which permits videotaping of engulfing sequences, followed by slow-motion playback for subsequent analysis. Particle and front velocities can be measured by timing their respective motions against a reference graticule of known dimensions.

There are two levels to this approach:

1. Level 1

The first level of the technique consists of the "ranking" of the coal particles in comparison with the liquid-vapour interfacial tension, γ_{LV}, of the organic matrix materials. At low solidification rates the surface tension forces are dominant and viscous drag and other forces are negligible. The detailed thermodynamic analysis shows [40] that in the case of $\gamma_{LV} > \gamma_{SV}$ (which is the case for all organic matrix materials studied so far) engulfing occurs for $\gamma_{LV} > \gamma_{PV}$ and rejection for $\gamma_{PV} > \gamma_{LV}$. Therefore, experiments with matrix materials of different surface tensions, γ_{LV}, (cf. Table 5/a) determine a lower and upper limit for the particle surface tension, γ_{PV}. Experimentally, all that is required is the observation whether or not coal particles, embedded in the melt of the matrix material, are engulfed or pushed by the slowly moving solidification front (solidification rates $\leq$ 1 µm/sec). Typical results for three different bituminous coals are given in Table 5/b. A detailed quantitative description of all the matrix materials used in Table 5 is contained in Ref [32]. The results given for the surface tension, γ_{PV}, of the coal particles and the corresponding calculated contact angle, θ, which water would form on ideally smooth surfaces of these coals are given for the melting point of the matrix materials. We found that $\frac{d\gamma_{PV}}{dT} \approx 0.07$ (mJ(m^2°C)) is a good estimate for the temperature of coefficient of

the surface tension of these coals [41]. Therefore, γ_{PV} and θ values can be readily estimated for other temperatures. We note already here that the surface tension of coal is in many cases near 40 mJ/m^2, coal No. 3 in Table 5 is a notable exception, being much more hydrophobic.

2. Level 2

In cases where particles are rejected (pushed), as the rate of solidification is increased, viscous drag on the particle will also increase and eventually lead to engulfment overcoming the resistance due to a positive ΔF^{adh}. In such situations engulfing occurs at a limiting rate of solidification called the critical velocity of engulfment, V_c. The critical velocity is determined through microscopic observation of the behaviour of particles at the advancing front as the rate of solidification is increased. At V_c the repulsive force, due to a positive ΔF^{adh}, and the retarding forces acting on the particle, are equal and engulfment results from any small disturbance.

From a large body of experimental data, giving V_c as a function of particle size, the free energy of adhesion was related to V_c through a scheme of dimensional analysis [33]. For particles less than 300 μm in diameter the relationship between ΔF^{adh} and V_c is given by the following equation:

$$\Delta F^{adh} = 6.07 \times 10^{3} \frac{\rho_L^{0.685} T^{0.400} k_p^{0.601}}{\mu^{0.085} (\rho_p \cdot C_p)^{0.201}} D^{0.484} V_c^{0.685} \qquad (9)$$

where the individual terms are in S.I. units and are:

ρ_p: particle density

ρ_L: liquid matrix density

C_p: heat capacity of the particle per unit mass

k_p: thermal conductivity of the particle

μ: viscosity of the liquid matrix

T: melting temperature of the matrix material

D: particle diameter

V_c: critical velocity

The experimental data consist of many individual observations of the distance a particle is pushed and the corresponding particle and solidification front velocities [31,33]. The aim of these observations is to determine the critical velocity of engulfment, V_c. At the critical velocity these forces are equal and engulfment is produced by any small disturbance. Fig. 4 presents the experimental data for particles of a bitumenous coal suspended in a matrix of thymol. This figure plots the rate of solidification, V, versus particle diameter, D. There are three modes of particle-solidification front interaction, distinguished by different symbols and referred to as "rejection", "transition", and "engulfment". The data are divided into these three regimes according to the distance of particle pushing. If the particle is pushed by the advancing solidification front by a distance greater than approximately 20 μm, i.e. continuously, the event is classified as a "rejection". If the particle is pushed a distance less than 20 μm the event is recorded as a "transition" and if engulfment occurs without significant pushing (less than 2 μm) by the solidification front the event is classified as an "engulfment". These are somewhat arbitrary classifications, but it should be noted that the determination of the "critical velocity" is not significantly dependent on any single observation. On average, over 200 separate observations of particle-front interactions are recorded in order to determine the V_c of each particle type. The identification of these three modes of particle-front interactions reflects the fact that the transition from "rejection" to "engulfment" is not

sharp. There are instances where the particle, when encountered by the solidification front, is reorientated and transported a short distance before being engulfed. In all cases, at very low velocities there is 100% rejection (pushing) and at very high velocities there is 100% engulfment. Clearly, between these extremes must be the critical velocity, V_c, where the process of particle pushing (rejection) gives way to that of particle engulfment.

The transition velocities correspond to velocities just above that of the highest rejection velocity. Pushing distances at V_c are extremely short since the slightest disturbance (e.g. turbulence, friction, thermophoretic effects, particle reorientation) in the balance of the opposing forces will produce immediate engulfment.

Since particle size influences the critical velocity, it is necessary to plot the experimental velocity observations of rejection, transition and engulfment as a function of particle size as shown in Fig. 4. The upper line of this plot is drawn so that above this curve no further transition points are noted; similarly, the lower line is drawn so that below this curve no further transition points are noted. Thus, this band encompasses the largest possible error. From this large body of experimental data it is thus possible to obtain V_c as a function of particle size, D, as the line that is equidistant from the two lines described above. In the summary plot contained in Fig. 5, the critical velocity, V_c, <u>versus</u> particle diameter, D, obtained from the measurements with three matrix materials (thymol, biphenyl and naphthalene) for a different coal sample, i.e. "coal No. 2", are plotted.

As the physical properties (cf. Equation (9)) of the various matrix materials are known or can be determined experimentally, it is thus possible, using V_c data, to calculate ΔF^{adh} through the use of Eq. (9). Having

thus obtained a value for ΔF^{adh}, it is possible, through the use of the equation of state approach [7] to obtain the various relevant interfacial tensions contained in Eq. (8) and in this manner determine the surface tension, γ_{pv}, of the small particles. Thus, the sequence of steps required to obtain the surface tension, γ_{pv}, of the particles may be summarized as follows:

$$V_c \rightarrow \begin{matrix}\text{Dimensional analysis} \\ \text{through Eq. (9)}\end{matrix} \rightarrow \Delta F^{adh} \rightarrow \begin{matrix}\text{Equation of state for} \\ \text{interfacial tensions}\end{matrix} \rightarrow \gamma_{pv}$$

Such γ_{pv} determinations, however, require a prior knowledge of the liquid-vapour, γ_{LV}, and the solid-vapour, γ_{SV}, surface tensions of the respective matrix materials. The γ_{LV} values can be obtained experimentally using conventional methods, such as the Wilhelmy plate technique [14]. The solid surface tension, γ_{SV}, may be determined through contact angle measurements and the equation of state approach [7] as discussed earlier in Section 2. As contact angle measurements at the melting point of the matrix material are not feasible, these measurements have to be performed as a function of temperature at temperatures below the melting point [32]. The data at the melting point can then be obtained by extrapolation. An appropriate method for such temperature dependent contact angle measurements is the technique of capillary rise at a vertical plate [42].

From the critical velocity data of Fig. 5, coal particle surface tensions, γ_{pv}, were calculated and plotted in Fig. 6 as a function of particle diameter; similarly, the contact angles which water would form on an ideally smooth surface are given in Fig. 7.

Ideally, one would expect that the measurements with the three different matrix materials would all produce identical values of γ_{pv} as well as θ. This is not the case. By comparison, similar data for polymer particles give

very good consistency, suggesting that the pattern of Figs. 6 and 7 is due, at least in part, to the well-known complexities of coal. Some of the difficulties of applying the technique to coal fines were discussed in Ref. [41]. On the other hand, recalling that the accuracy of contact angle measurements on well prepared polymer surfaces by means of the sessile drop technique is commonly given as $\pm$ 2° the agreement in Fig. 7, at least for small particles, is entirely satisfactory. The data of Figs. 6 and 7 also suggest a dependence of particle surface tension on particle size. This finding is quite general for coal particles [27,41,43]. The observed increase in hydrophobicity with decreasing particle size corresponds well with the well-known percentage decrease of inorganic matter in the coal. Particle size dependencies, such as those observed in Figs. 6 and 7, are indeed not observed for polymer particles [43]. Surface tension values for a number of different coals are given for 60 µm diameter particles at 20°C in Table 6. It is to be noted that the surface tension of many coals seems to be near 40 mJ/m^2. Note, however, coal No. 1 in Table 5 which is markedly more hydrophobic.

One of the main strengths of this technique is its extreme sensitivity. As an illustration, we present in Figs. 8 and 9 V_c and θ data, respectively, for two identical coal samples, the only difference being that for one set of measurements the coal fines were dry screened and wet screened for the other. At first sight, it is surprising that the wet screened sample is slightly more hydrophobic than the dry screened sample. The explanation lies in the removal of inorganic matter in the wet screening process [41].

Freezing front experiments can be performed not only with organic matrix materials, but with water/ice as well. Thermodynamically, there is one significant difference between the organic matrix materials and water/ice: For the

former we have $\gamma_{SV} < \gamma_{LV}$, whereas for the latter $\gamma_{SV} > \gamma_{LV}$ holds. As a consequence it is those particles for which $\gamma_{PV} < \gamma_{LV}$ which are being rejected and pushed by the solidification front.

As an illustration, a typical plot of solidification front velocity versus particle diameter [44] is given in Fig. 10. The corresponding plots for other coal samples are quite similar. The interfacial tension values, γ_{PV}, for a different type of coal (No. 3, subbituminous), are given in Fig. 11, together with the results obtained with an organic matrix material, thymol. There is a marked difference of approximately 30 mJ/m^2 in the surface tension values obtained with the two types of matrix materials. In the presence of water the coal is markedly more hydrophilic with a surface tension near that of water. This striking difference suggests that one and the same coal sample may have two effective surface tensions or even a range of surface tensions, depending on the suspending liquid. It is likely that in water the coal particles acquire a thick hydration layer so that they are perceived by other phases present essentially as "black water particles". The fact that the particle size dependence, exhibited in thymol, has also vanished supports this contention. The comparison between thymol and water data (cf. Table 7) for three different coal samples [44] suggests that the pattern is quite general.

3.2.2. Sedimentation Volume

In the solidification front technique there were two types of situations: At very low rates of solidification the particles were either engulfed, indicating negative values of ΔF^{adh} and ΔF^{eng}, or they were pushed along by the solidification front, indicating positive values of ΔF^{adh} and ΔF^{eng}. In the case of an interaction between particles of the same kind, embedded in a liquid, this interaction is governed by the free energy of cohesion

$$\Delta F^{coh} = - 2 \gamma_{PL} \qquad (10)$$

As solid-liquid interfacial tensions are always positive or zero, as a limiting case [45], it follows that $\Delta F^{coh} \leq 0$, implying that there will, in the absence of electrostatic forces, always be an attraction between like particles suspended in a liquid (with no interaction as a limiting case, at $\gamma_{PL} = 0$).

To illustrate this point, we plot in Fig. 12 the free energy of cohesion, ΔF^{coh}, against the liquid surface tension, γ_{LV}, for hypothetical particles having a surface tension $\gamma_{PV} = 20$ mJ/m^2. It is apparent that a mimimum in ΔF^{coh} occurs at $\gamma_{LV} = 20$ mJ/m^2, suggesting that in a sedimentation volume experiment one should observe an extremum in the sedimentation volume at that point.

As sedimentation studies have long been a means of studying suspension stability, it is of interest to perform sedimentation experiments from the above perspective. As it is apparent from Eq. (5) that $\gamma_{PL} = 0$ when $\gamma_{LV} = \gamma_{PV}$, it is important to generate conditions under which this holds. In order to be able to control and vary the surface tension of the suspending liquids, binary mixtures of pairs of liquids may be chosen such that one of the pure liquids has a lower and the other a higher surface tension than the particles.

It is interesting to speculate on what might happen to the sedimentation volume in the special case when $\gamma_{LV} = \gamma_{PV}$. There are at least two possible patterns of behaviour, depending on whether or not agglomeration of the particles at early stages of sedimentation is possible.

a) If there is no agglomeration at finite values of the free energy of cohesion, then for zero free energy of cohesion least close packing of the sediment and hence a maximum in the sedimentation volume, V_{sed}, is expected.

b) If there is agglomeration at finite values of the free energy of cohesion at early stages of sedimentation, then this agglomeration would cease when the free energy of cohesion approaches zero. Since the irregularly shaped aggregates resulting from agglomeration do not pack well, one would expect minimum sedimentation volume at zero free energy of cohesion.

On the basis of these possible mechanisms, it appears that either a maximum or a minimum in the sedimentation volume would indicate $\gamma_{LV} = \gamma_{PV}$. Thus, by determining that liquid surface tension, γ_{LV}, for which the sedimentation volume assumes an extremum we determine in fact the particle surface tension, γ_{PV}. Maxima as well as minima in the sedimentation volumes have indeed been found for polymer particles [36,46] as well as coal fines [47].

Experimentally the final sedimentation volume, V_{sed}, which a fixed mass of coal particles suspended in a known volume of a liquid of known (i.e. measured) surface tension makes, is determined. For this purpose, graduated Wintrobe® tubes may be employed which allow V_{sed} readings with an accuracy of 0.01 ml. These tubes have a maximum capacity of 1.0 ml. The mass of coal particles best used in these studies depends on the nature of the particles themselves. Particle density, shape, size and size distribution all contribute to the final V_{sed} value. Since in this type of study one is not concerned with the absolute size of V_{sed} in the various tubes but rather is attempting to determine the relative position of the V_{sed} extremum as a function of the surface tension, γ_{LV}, of the suspending liquid, it is not necessary to use the same fixed mass of particles for different systems. For any single system, however, it is important that the same mass of particles always be suspended in each of the different liquid mixtures. Once the particles are introduced into the liquids, the suspension is vigorously shaken in

order to remove any entrapped air bubbles. The tubes are then sealed to prevent evaporation of the liquid and the particles are allowed to settle, under the influence of gravity, in the graduated tubes. The final V_{sed} values are thus determined as a function of the surface tension, γ_{LV}, of the suspending liquid.

The various γ_{LV} values required may be produced through the use of different homogeneous organic liquids such as a homologous alkane series [46] each of which has a unique surface tension, or a range of γ_{LV} may be produced through the use of binary mixtures, at various volume/volume concentrations, of two liquids, one of which has a high surface tension and the other a low surface tension. One example is n-propanol/water mixtures which would provide a wide γ_{LV} range from 23.8 to 72.8 mJ/m^2 at 25°C. There are several conditions which the suspending liquids must satisfy in order to be suitable for sedimentation volume experiments. The criteria for choosing liquid components are:

(1) they should be chemically inert with respect to the coal samples and should not dissolve the particles or components thereof;

(2) the boiling temperature should be reasonably high to minimize evaporation;

(3) the density of the liquids should be less than that of the particles;

(4) the surface tension, γ_{LV}, of the liquid mixtures should cover the surface tension range required.

In the case of coal the first criterion could introduce complications and should be kept in mind.

As an illustration of this technique we show in Fig. 13 a photograph of the sedimentation volume of Teflon particles [36] in binary mixtures of

n-hexane/n-hexadecane. The two outside cylinders contain pure n-hexane and pure n-hexadecane, respectively, and the other cylinders binary mixtures of different composition so as to span the surface tension range from γ_{LV} = 18.3 mJ/m^2 (n-hexane) to γ_{LV} = 27.0 mJ/m^2 (n-hexadecane), including the surface tension of 20 mJ/m^2, the known surface tension of Teflon.

The sedimentation volumes of Fig. 13, together with the sedimentation volumes of the same Teflon powder in binary mixtures of diethyl ether/tetralin and diethylether/n-hexanol, respectively, are plotted in Fig. 14 against the surface tension of the suspending liquids. It turns out that in all three cases there is an extremum near γ_{LV} = 20 mJ/m^2, in keeping with the thermodynamic expectations. It is apparent that such sedimentation experiments may be used to determine the surface tension of small particles. The question when a maximum or a minimum is observed, while not completely resolved at this time, does not interfere with the application of the technique. It appears that minima are observed in more non-polar liquids and maxima in more polar liquids.

The sedimentation volume technique has been applied to the study of the surface tension of several coal fines [47]. Typical results are given in Fig. 15 for one and the same coal and four different types of binary mixtures. On the one hand, one might say that the position of the extremum is reasonably constant from one binary mixture to the next. On the other hand, the trend to lower values of γ_{PV} for the more polar liquid mixtures is unmistakable. The reason for this is not yet known. The trend to lower values of the extremum for the more polar liquids is not universal. For a different coal sample the opposite trend was found, see Table 8.

The dependence of surface tension of the coal fines on particle size can also be studied by means of the sedimentation volume technque. For the B.C. coal sample studied in Fig. 15, the particle size dependence was studied for binary mixtures of n-propanol/ethylene glycol, see Fig. 16. We infer that the position of the maximum shifts from approximately 28 mJ/m^2 for the smallest particles to 44 mJ/m^2 for the largest particles. This variation, while in the expected direction, is surprisingly large. As solidification front experiments with the same coal in thymol have also been performed, the results of the two techniques are compared in Table 9. A comparison for a second coal, originating from Wabamun Lake, is also given in Table 9. For both coals the spread of surface tension is much smaller in the case of the solidification front technique. However, for the larger particles the agreement between the two techniques for both coals is remarkable. Pragmatically, we are inclined to give more credence to the freezing front technique, because of our more extensive experience with it.

The sedimentation volume technique has also been used to study the dualistic behaviour of coal with respect to organic media and water [47], which was discussed above in connection with the solidification front technique. To illustrate, at the same time, the reproducibility of sedimentation volume measurements, the results of two identical experiments in mixtures of dimethyl sulfoxide (DMSO) and water are given in Fig. 17. It is inferred that the surface tension of the coal particles is approximately 69 mJ/m^2, in good qualitative agreement with the solidification front result, see Table 11.

The sedimentation experiments yielding the low value of γ_{pv} were all performed in non-aqueous media. It is an interesting question whether it is the presence of water <u>per se</u> which gives the coal a hydrophilic character or

whether the surface tension of the liquid, no matter how it arises, determines the sedimentation behaviour. Therefore sedimentation experiments were performed with a frequently studied coal, Pittsburgh No. 8, in aqueous mixtures of n-propanol, over the entire range of surface tension from γ_{LV} = 23.8 mJ/m^2 (n-propanol) to γ_{LV} = 72.5 mJ/m^2 (water). The resultant curve [48] in Fig. 18 exhibits two maxima, suggesting that coal has the property to be hydrophobic as well as hydrophilic in binary mixtures of the same two components.

3.2.3. Particle Adhesion

The pattern of behaviour of particles interacting with solidification fronts suggests that the free energy of adhesion, ΔF^{adh}, as given by Eq. (8), may also govern the adhesion of particles, out of a liquid, to any solid surface, not just to solidification fronts. The thermodynamic model for particle adhesion, as implied in Fig. 1 and Eq, (8) predicts patterns of behaviour considerably more complex than might be expected. As an illustration, we show in Fig. 19 the calculation of the free energy of adhesion (ΔF^{adh}) for the adhesion of particles as a function of varying substrate surface tension, γ_{SV}, for the two cases where the liquid surface tension, γ_{LV}, is either smaller or larger than the surface tension, γ_{PV}, of the adhering particles themselves. For the case where

$$\gamma_{LV} > \gamma_{PV} \qquad (11)$$

ΔF^{adh} increases with increasing γ_{SV} (increasing substrate hydrophilicity), thus predicting a decreasing extent of particle adhesion with increasing substrate surface tension, γ_{SV}, over a wide range of γ_{SV} values. On the other hand, when

$$\gamma_{LV} < \gamma_{PV} \qquad (12)$$

the opposite pattern of behaviour is predicted; i.e. increasing particle adhesion with increasing γ_{SV} corresponding to a decreasing ΔF^{adh} with increasing γ_{SV}. For the limiting case where

$$\gamma_{LV} = \gamma_{PV} \tag{13}$$

ΔF^{adh} becomes equal to zero independent of the value of the substrate surface tension, γ_{SV}. The relations (11) - (13) suggest that particle adhesion to one and the same substrate could be drastically different for different surface tensions of the suspending liquid medium. As an illustration we show, in Fig. 20, photomicrographs of the extent of adhesion of Devco coal particles to a hydrophobic and a hydrophilic polymeric substrate, out of a high and a low surface tension liquid, respectively. We note that the relative amount of particles adhering to the two solid substrates is indeed reversed as the surface tension of the liquid is changed.

Figure 20 in conjunction with relations (11) - (13) suggests a strategy of how to determine the surface tension of the particles from such observations of particle adhesion: We have to adjust the liquid surface tension to such a value that the extent of particle adhesion becomes equal on different solid substrates. The surface tension of the particles will then be equal to the known surface tension of the suspending liquid medium. This condition is best established by determination of the extent of particle adhesion to a range of solid substrates, out of suspensions having also a suitable range of surface tension.

As a typical example, the relative extent of particle adhesion is plotted in Fig. 21 over the surface tension of the various solid substrates used, for a number of different suspending liquids differing in their surface tension (experimental details will be given below). While there is considerable

scatter in the experimental data, the least squares fitted straight lines are in general agreement with the thermodynamic model, as expressed in Fig. 19. For the highest liquid surface tension the slope of the straight line is large and negative, decreases with decreasing liquid surface tension and becomes finally positive.

The precise value of the surface tension of the particles can be readily determined from a plot of the slopes of the straight lines in Fig. 21 over the liquid surface tension, as given in Fig. 22. The intercept of this plot with the γ_{LV} axis represents the case of Eq. (13), i.e. this intercept is equal to the surface tension, γ_{PV}, of the particles.

The scatter of the data in Fig. 21 is a consequence of the heterogeneous nature of coal. The adhesion technique was actually developed as a means of determining the surface tension of biological cells [37,38]. For such systems there is very little scatter. It is interesting to note that the curvature at low γ_{SV} values in the theoretical curves of Fig. 19 are not apparent in Fig. 21, nor in any of the results with biological cells [37,38].

On the experimental side, the adhesion technique relies on determining the extent of the adhesion of particles to polymer surfaces of varying surface tension when suspended in liquids of various surface tensions. Thus from an experimental standpoint the following is required: A means of preparing a number of different substrate materials with a wide range of known surface properties; a means for quantitating the number of particles adhering per unit surface area for each substrate material; and a means for measuring the surface tensions of the various suspending liquids.

We routinely employ the polymer surfaces listed in Table 10 as suitable substrate materials for particle adhesion studies. These polymers, with the

exception of polystyrene and sulphonated polystyrene, are prepared by heat pressing. Detailed methodology for producing suitable surfaces are available from the authors upon request. Following preparation, all of the substrates should be examined for surface defects, e.g. surface roughness, and their surface properties characterized by means of contact angle measurements (cf. Table 10). Any surface which exhibits roughness or incorrect contact angle values should be discarded.

In order to produce liquids of varying surface tensions binary mixtures are prepared from two liquids, one with a high surface tension and the other with a low surface tension. For this purpose water (high surface tension) and propanol, dimethyl sulfoxide, ethylene glycol have been used previously [37,38,49]. Propanol has the advantage that small concentrations produce a marked lowering of the surface tension of the mixture. Propanol also has an added advantage over the other alcohols in that it has a low vapour pressure. The main selection criterion is the fact that a range of liquids is chosen the surface tensions of which are partly higher and partly lower than the surface tension of the particles of interest; furthermore the liquids should not dissolve neither the particles or substrates. The surface tensions of the suspending liquids may be measured by any of a number of techniques, e.g. Wilhelmy Balance Method.

In order to hold the particle suspension in place it is retained in wells bored into Teflon moulds. The mould is clamped onto the polymer surface and leakage is prevented through the use of silastic rubber gaskets. Before each experiment, the Teflon moulds are sonicated in methanol and then rinsed in deionized, distilled water. Each mould has three wells allowing measurement in triplicate.

The experiment proper is performed as follows: A fixed volume of particle suspension (at a known concentration) is pipetted into the center of each well. The system is then checked for leaks and sealed with Parafilm to prevent evaporation. The particle suspension is left in place for a fixed period of time at the desired temperature. The incubation period is predetermined from a series of kinetic studies as illustrated in Fig. 23. It is our routine procedure to use a time-point which is located on the plateau region. Thereafter, the mould with the attached surface is immersed in a bath of the same liquid used to suspend the particles. Whilst immersed, the Teflon mould and silastic gaskets are removed. (Removal of the mould and gaskets <u>whilst</u> immersed is not a trivial step and needs to be performed in order to ensure reproducibility of experimental data).

The surfaces are then air dried and the number of particles adhering per unit area of polymer material is determined. For this purpose we employ an automatic image analysis system which can be programmed to determine either the number of particles per unit area or the fraction of area covered by the particles. With irregularly shaped particles, such as coal fines, the latter strategy is preferable. To date three types of coal fines have been studied, and only in aqueous media [49]. The results are summarized in the last column of Table 11.

IV. DISCUSSION

4.1. Comparison of the Results Obtained by Different Techniques

Table 11 contains the results for four coals, for which measurements were performed with at least three of the four techniques discussed, i.e. direct contact angle measurement, solidification front, sedimentation volume and adhesion technique. Disregarding for the moment the direct contact angle

measurements the most striking conclusion is that coal does not have a unique surface tension. In organic media the surface tension is roughly in the range of 30-40 mJ/m^2 and in aqueous media much higher, near the surface tension of water (72.5 mJ/m^2). In this respect coal is markedly different from homogeneous materials such as polymers, for which the available evidence suggests that the surface tension is indeed unique. The fact that the surface tension for the four coal types turns out to be almost identical in the solidification front technique with water suggests that the coal particles will be highly hydrated making the coal particles virtually "black water particles", as far as surface properties are concerned. This interpretation is supported by the finding that there is, in water, no more particle size dependence, see, e.g., Fig. 11.

Comparison of the results for solidification front, sedimentation volume and adhesion technique, in the case of aqueous media, shows remarkable agreement for the B.C. and Devco coal samples, but not for the Coal Valley and coal No. 3 samples. For the latter two samples there is a high content of inorganic matter which might interact preferentially with the non-aqeuous component in the binary liquid mixtures in which sedimenatation and adhesion experiments are performed, in such a way as to make the particles more hydrophobic.

With respect to the organic media, solidification front data for the coal particle surface tension turn out somewhat larger than sedimentation volume results, for the particle size fraction considered, i.e. particles smaller than 30 μm. Recalling, however, Table 9, we note that for larger particles the agreement between solidification front and sedimentation volume is very good, in the two cases for which particle size dependence has been performed with the sedimentation volume method. The extremely small values obtained for

the small particles by means of the sedimentatation volume technique, in conjunction with the fact that the solidification front data are consistently higher suggests that there might be some as yet unidentified artefact connected with the sedimentation volume data. It should be noted that these complications are not primarily of a methodological nature, but are due to the complexities of coal. No such size effects are known for polymer particles.

Turning finally to the contact angle results in the first two columns of Table 11, we note first of all that the advancing contact angles reported in Table 3 with water as measuring liquid do not yield the high surface tension values observed with the solidification front, sedimentation volume and adhesion technique, when applied with aqueous media. In the case of B.C. and Devco coal there is indeed remarkable agreement with the solidification front results. This pattern is surprising only at first sight. It is well known that the advancing contact angles are a measure of the low energy portions of a heterogeneous solid surface [28], in our case the organic components of the coal surface. For this reason it also makes good sense that the results of the contact angle measurements come out equal to those of the small and not the larger particles, as the larger particles contain generally more inorganic impurities.

The contact angle results for the Coal Valley sample are probably meaningless. This coal has a very high mineral content and photomicrographs of polished sections show bands of clay. It seems likely that sessile drops will spread along such channels, making the observed contact angle smaller than what it would be in the absence of such channels, and the surface tension larger. The surface tension results with organic liquids turn out smaller than those obtained with water and do not agree with any of the other measurements. This

also is in contradistinction to the behaviour of homogeneous organic solids, where, on well-prepared surfaces, the surface tension turns out to be independent of the measuring liquid.

In conclusion, we feel that there is a wealth of useful information to be obtained through comparisons such as in Table 11, but we do not, as yet, understand all aspects of the patterns of coal behaviour.

4.2. Applicability and Range of Validity of the Different Techniques

Table 12 summarizes some of the advantages and limitations of the techniques described in this article.

The direct contact angle approach, whilst being the easiest to perform, has only a limited scope. This is particularly so due to the difficulties with polishing the coal sample. The primary concern here is that the polished surface, even if it allows the determination of a thermodynamically meaningful contact angle, may differ from the natural, i.e. unpolished surface. Secondly, the entire question of "smoothness" as related to contact angle measurements on coal has yet to be resolved.

In this regard the adhesion, sedimentation volume and advancing solidification front techniques offer a real advantage, as they permit the study of coal particles in any state. These techniques suffer from the drawback that they can only be applied to relatively small coal particles less than 200 or possibly 300 μm in major diameter.

Of these methods the most easily employed is the sedimentation volume method, owing to its simplicity of operation and inexpensive nature. In contrast to the other two techniques, however, it lacks a high degree of precision.

The adhesion technique exhibits a high degree of sensitivity and is able to detect differences in wettability of only 0.5 mJ/m^2. The technique, however, requires the laborious and careful preparation and prior surface characterization of the polymer substrates. In addition, in the case of coal where the particles are irregular in both shape and size and adhere such that individual particles are not readily identifiable, it is necessary to employ sophisticated image analysis systems to quantitate the extent of particle adhesion.

The advancing solidification front technique, whilst also requiring fairly sophisticated equipment, has the distinct advantage of exhibiting remarkable sensitivity to only very small differences in the wettability of the particles examined. For example in the case of naphthalene as the matrix material, a 1 mJ/m^2 difference in surface tension corresponds to a difference in critical velocity of approximately 40 μm/sec i.e. an order of magnitude larger than the readily attainable accuracy of the measurement.

V. APPENDIX

5.1. List of Symbols

A	surface area
C_p	specific heat of the particle
D	particle diameter
ρ_L	density of the liquid matrix material
ρ_P	density of the particle
ΔF^{adh}	free energy of adhesion
ΔF^{coh}	free energy of cohesion
ΔF^{eng}	free energy of engulfment
k_P	thermal conductivity of the particle
$N_i^{(A)}$	number of moles of component i in the surface
γ	surface tension
γ_S	surface tension of solid
γ_{SV}	solid/vapour interfacial tension
γ_{SL}	solid/liquid interfacial tension
γ_{LV}	liquid/vapour interfacial tension
γ_{PV}	particle/vapour interfacial tension
γ_{PL}	particle/liquid interfacial tension
γ_{PS}	particle/solid interfacial tension
$\frac{d\gamma_{PV}}{dT}$	temperature coefficient of the particle surface tension
μ	viscosity of the liquid matrix material
$S^{(A)}$	surface entropy
T	melting temperature of the matrix material
θ	contact angle
θ_A	advancing contact angle
θ_R	receding contact angle
$U^{(A)}$	surface energy
V	solidification front velocity
V_c	critical velocity of engulfment
V_{sed}	sedimentation volume

5.2. Characterization of Coal Samples Discussed

The origin, rank, type of sizing and density of coal samples referred to in this chapter are summarized in Table A1. For coals most frequently used as examples in this article, such as B.C., Devco and coal No. 3, both the proximate and the ultimate analysis data are given in Tables A2, A3 and A4, respectively, for the different fraction sizes. The proximate analysis results for the -400 mesh fractions of the Pittsburgh No. 8 and the Coal Valley samples as well as the ultimate analysis data for the same size fraction of the Pittsburgh No. 8 coal are summarized in Table A5.

Table 1

Suggested Selection Criteria for Suitable Coal Sample for Measuring Contact Angles on Coal Segments

1.	Sample should be free of cracks or mineral occlusions.
2.	Major bright area (vitrain) or other lithotypes should be selected.
3.	Sample should be representative of bulk coal specimen from a petrographic and chemical aspect.
4.	Proximate and ultimate chemical analysis should be available.
5.	Surface of cut specimmens should be polished to obtain smooth surfaces.
6.	Sample should be rigid.

Table 2

Contact Angle, θ, Measured on Teflon Surfaces of Different Roughnesses and the Apparent Surface Tension, γ_{SV}, of Teflon Calculated from the Contact Angles

	Contact angle, θ (degrees)			Surface tension, γ_{SV} (mJ/m^2)		
Surface finish	Ethylene glycol	Glycerol	Water	Ethylene glycol	Glycerol	Water
Roughened surface 220 grit	133.0	-	155.2	2.2	-	0.6
Roughened surface 600 grit	99.5	-	121.8	11.3	-	9.7
Smooth surface (from Ref [32])	81.0	96.0	104.0	20.0	19.6	20.0

Table 3

Mean Values of Contact Angles, θ, Obtained with Organic Liquids and with Water on Segments of Coals with Different Surface Finishes at 20°C

Surface finish	Contact angle, θ (degrees)								
	B.C. Coal			Devco coal			Coal Valley coal		
	Ethylene glycol	Glycerol	Water	Ethylene glycol	Glycerol	Water	Ethylene glycol	Glycerol	Water
Surface as cut	33.9±0.5	69.9±1.1	84.4±1.0	47.8±1.4	69.1±1.1	78.8±2.0	22.8±0.8	43.1±1.9	38.2±0.8
Rough polish 220 grit	39.5±0.7	59.6±1.0	76.4±1.4	39.4±0.9	77.1±0.7	71.3±2.9	21.9±1.6	36.8±1.6	44.0±1.2
Medium polish 600 grit	42.8±1.5	65.0±0.7	77.8±1.1	50.3±0.9	77.5±0.6	75.3±2.3	28.9±1.3	40.4±2.4	44.4±1.5
Fine polish Nylon cloth	41.5±0.9	72.2±1.0	76.4±1.1	49.4±1.3	83.9±2.0	68.8±1.4	26.7±2.0	55.7±1.1	45.1±0.8
Fine polish Microcloth	49.6±0.5	75.6±1.0	77.3±0.8	57.2±0.9	83.8±0.6	76.8±1.2	28.6±0.7	53.1±1.2	47.5±3.9

Table 4

Surface Tension Values, γ_{PV}, Obtained with Organic Liquids and with Water on Segments of Coals with Different Surface Finishes at 20°C from the Contact Angle Data Listed in Table 3

Surface finish	Surface tension, γ_{PV} (mJ/m2)								
	B.C. Coal			Devco coal			Coal Valley coal		
	Ethylene glycol	Glycerol	Water	Ethylene glycol	Glycerol	Water	Ethylene glycol	Glycerol	Water
Surface as cut	40.5±0.2	33.9±0.6	32.5±0.6	34.5±0.6	34.4±0.6	36.0±1.2	44.3±0.3	49.0±1.0	60.0±0.5
Rough polish 220 grit	38.2±0.3	39.8±0.6	37.5±0.9	38.1±0.4	30.0±0.4	40.7±1.7	44.6±0.6	52.3±0.8	56.7±0.7
Medium polish 600 grit	36.8±0.6	36.7±0.4	36.7±0.7	33.4±0.4	29.7±0.3	38.1±1.4	42.3±0.5	50.4±1.2	56.5±0.9
Fine polish Nylon cloth	37.3±0.4	32.7±0.6	37.5±0.7	33.8±0.6	26.3±1.1	42.2±0.8	43.1±0.7	42.0±0.6	56.1±0.5
Fine polish Microcloth	33.7±0.2	30.8±0.6	37.0±0.5	30.1±0.4	26.3±0.3	37.3±0.7	42.6±0.2	43.5±0.6	54.7±2.3

Table 5/a

Melting Points and Surface Tensions, γ_{LV}, of the Liquid Organic Matrix Materials at the Melting Point

Matrix material	Melting point °C	Surface tension, γ_{LV} at melting point (mJ/m^2)
Thymol	51.5	29.9
Biphenyl	70.0	32.5
Naphthalene	80.5	32.8
Salol	43.0	35.3
2-Phenyl phenol	59.0	38.7

Table 5/b

Results and Conclusions Regarding the Ranking Series of Engulfing Experiments for Coal Samples from Level 1 Investigations

Coal sample	Experimental observations	Surface tension, γ_{LV} (mJ/m^2)	Contact angle of water, θ (degrees)
No. 1	Engulfed by all matrix materials	$\gamma_{PV} < 29.9$ at 51.5°C	$\theta > 82.7$ at 51.5°C
No. 2	Rejected by thymol, biphenyl, naphthalene, salol Engulfed by 2-phenyl phenol	$\gamma_{PV} > 35.3$ at 43°C $\gamma_{PV} < 38.7$ at 59°C	$\theta < 75.3$ at 43°C $\theta > 65.7$ at 59°C
No. 3	Rejected by all matrix materials	$\gamma_{PV} > 38.7$ at 59°C	$\theta < 65.7$ at 59°C

Table 6

Particle Surface Tensions, γ_{pv}, from Solidification Front Experiments in Organic Matrix Materials for Various Coal Samples; γ_{pv} are Given for 60 μm Particle Size

Coal sample	Rank	Type of sizing	Matrix material	γ_{pv} at 20°C (mJ/m^2)
No. 2	bituminous	wet screened	thymol	40.8 ± 1.1
			biphenyl	39.0 ± 0.3
			naphthalene	39.4 ± 0.4
Devco	bituminous	dry screened	thymol	39.7 ± 1.0
Minto	bituminous	dry screened	thymol	39.8 ± 1.1
B.C.	bituminous	dry screened	thymol	41.5 ± 1.4
Cardinal River	bituminous	dry screened	thymol	42.0 ± 1.9
Coal Valley	bituminous	dry screened	thymol	40.3 ± 0.9
Denison	bituminous	dry screened	thymol	39.0 ± 1.0
Wabamun Lake	bituminous	dry screened	thymol	39.2 ± 1.0
No. 3	subbituminous	dry screened	thymol	39.5 ± 1.3
No. 3	subbituminous	wet screened	thymol	39.2 ± 1.5

Table 7

Surface Characteristics of Coal Samples from Solidification Front Experiments in Thymol and Water at 20°C; Data are Given for 30 μm Particle Size

	THYMOL		WATER	
Coal sample	V_c (μm/s)	γ_{PV} (mJ/m^2)	V_c (μm/s)	γ_{PV} (mJ/m^2)
B.C.	10.3 ± 2.4	38.7 ± 1.0	34.0 ± 2.5	71.8 ± 0.1
Devco	5.4 ± 1.4	36.4 ± 0.7	21.7 ± 3.2	72.1 ± 0.4
No. 3	8.7 ± 0.9	38.3 ± 0.5	6.3 ± 0.6	72.3 ± 0.1

Table 8

Extrema of Sedimentation Volumes, V_{sed}, for Coal No. 1 in Liquid Mixtures of Different Polarity

Liquid pairs used	Surface tension range γ_{LV} (mJ/m^2)	Dipole moment range $\mu \times 10^{-30}$ (Cm)	V_{sed} extremum at γ_{LV} of liquids	
			Type	γ_{LV} (mJ/m^2)
n-Octane/Decalin	21.8/32.3	0/0	min	28.4
Cyclohexane/Decalin	24.9/32.3	0/0	min	28.7
Benzene/Chlorobenzene	28.9/33.6	0/ 5.64	min	32.4
Benzene/1,2,4 Trichlorobenzene	28.9/39.7	0/ ?	min	33.1
Methanol/Ethylene glycol	23.5/48.9	5.67/ 7.61	max	33.4
Acetone/Ethylene glycol	22.6/48.9	9.61/ 7.61	max	34.6
Methanol/Formamide	23.5/59.9	5.67/12.44	max	33.9

Table 9

Particle Size Dependence of Surface Tension, γ_{pv}, of Coal Obtained from Solidification Front and Sedimentation Volume Techniques in Organic Media; Data Given Here are Mean Values of γ_{pv} Characteristic of the Relevant Mesh Fractions of Each Coal Sample

Coal sample	Mesh fraction	Particle surface tension γ_{pv} (mJ/m^2) at 20°C from	
		Solidification front (in thymol)	Sedimentation volume (in n-propanol/ ethylene glycol)
B.C.	-400 (D < 37 µm)	38.7	27.8
	-325 + 400 (37 µm < D < 44 µm)	40.2	31.5
	-200 + 325 (44 µm < D < 74 µm)	41.5	35.9
	-100 + 200 (74 µm < D < 149 µm)	43.6	44.0
Wabamun Lake	-400 (D < 37 µm)	36.9	31.5
	-325 + 400 (37 µm < D < 44 µm)	38.0	34.1
	-200 +325 (44 µm < D < 74 µm)	39.1	39.3

Table 10

Solid Substrates Used in the Coal Adhesion Experiments

Material	Source	Preparation	Contact angle of water (degrees)	Surface tension γ_{SV} (mJ/m^2)
Fluorinated Ethylene-propylene Copolymer (FEP)	Commercial Plastics Toronto, Canada	Heat Press	110 ± 3	16.4
Polystyrene (PS)	Central Research Lab. Dow Chemical Co.	Film	95 ± 2	25.6
Low Density Poly-ethylene (LDPE)	Commercial Plastics Toronto, Canada	Heat Press	84 ± 4	32.5
Polyethyleneterephthalate (PET)	Hoechst Canada Inc. Willowdale, Ontario	Film	60 ± 2	47.0
Sulfonated Polystyrene (SPS)	Central Research Lab. Dow Chemical Co.	Film	24 ± 3	66.7

Table 11

Comparison of the Surface Tension, γ_{SV}, of Coals Obtained from Contact Angles and from the Solidification Front, Sedimentation and Adhesion Techniques in Both Organic and Aqueous Media. Surface Tensions from Contact Angles are Averaged Results Obtained on Surfaces after Final Polishing with Microcloth; Data Obtained from the Other Techniques Refer to Size Fractions Below 30 µm.

Coal sample	Surface tension, γ_{SV} (mJ/m2), at 20°C						
	Contact angle		Organic Media		Aqueous media		
	Organic liquids	Water	Solidification front	Sedimentation volume	Solidification front	Sedimentation volume	Adhesion
B.C.	32.3	37.0	38.7	27.8-30.2	71.8	70.9	69.0
Devco	28.2	37.3	36.4	33.0-35.4	72.1	69.0	68.9
Coal Valley	43.1	54.7	37.5	31.0-35.9	72.2	63.3	-
No. 3	-	-	37.7	28.5-35.9	72.3	64.4	64.9

Table 12

Advantages and Limitations of the Various Techniques
Used for Determining the Surface Properties of Coal Particles

Method	Advantage	Limitation
Direct contact angle	a. Easy to perform b. Sample preparation is straightforward	a. Relatively large scatter in experimental data b. Thermodynamic status and significance of contact angles is unclear.
Solidification front	a. Readily applicable for large size range (from 5 to 300 μm) b. Small amount of particles required c. Very good reproducibility d. Extreme sensitivity	a. Lack of understanding mechanism in detail and theoretical complexities b. Requires a knowledge of the material properties of the particles c. Sophisticated instrumentation required
Sedimentation volume	a. Applicable to particles with a size range from 1 to 150 μm b. Simple and inexpensive method	a. Narrow particle size range is necessary b. Relative large amount of sample required c. Limited accuracy and sensitivity
Particle adhesion	a. Readily applicable to small particles (< 15 μm) b. Small amount of particles required c. High accuracy	a. Can only be employed for a narrow particle size range b. Time consuming c. Sophisticated instrumentation required

Table A1

Origin, Rank, Type of Sizing and Density of Coal Samples

Coal sample	Origin	Rank and date of mining	Type of sizing	Density ρ(kg/m^3)
No. 1	Quintette Area Northeastern British Columbia	bituminous medium-volatile 1979	wet screened	1520
No. 2	Mountain Park Area, Alberta	bituminous medium-volatile 1979	wet screened	1470
Devco	Sidney Nova Scotia	bituminous high-volatile 1982	dry screened	1370
Minto	New Brunswick	bituminous high-volatile 1982	dry screened	1357
B.C.	Kaiser Resources Harmer Seam Pit 29 South British Columbia	bituminous 1982	dry screened	1410
Cardinal River	Hinton Alberta	bituminous 1982	dry sceened	1320
Coal Valley	Mynheer A Seam Coal Valley Alberta	bituminous 1983	dry screened	1445
Denison	Denison Mine Quintette Area British Columbia	bituminous 1983	dry screened	1430
No. 8	Pittsburgh	bituminous	dry screened	1500
No. 3	Judy Creek Area Northern Alberta	subbituminous 1979	dry screened	1630
Wabamun Lake	Wabamun Lake Alberta	subbituminous 1983	dry screened	1400

Table A2

Proximate and Ultimate Analysis Data for Different Size Fractions of B.C. Coal (as received)

Mesh fraction	Proximate analysis				Ultimate analysis				
	Moisture	Ash	Volatile	Fixed carbon (diff.)	C	H	N	S (total)	O (diff.)
	(wt %)				(wt %)				
- 60+100	0.47	31.06	19.44	49.03	54.90	3.23	0.78	0.14	9.42
-100+200	0.43	23.55	20.13	55.89	60.19	3.52	0.76	0.20	11.35
-200+325	0.42	21.45	19.21	58.92	65.81	3.66	0.85	0.18	7.63
-325+400	0.38	19.65	19.13	60.84	67.04	3.74	0.89	0.20	8.10
-400	0.46	15.37	20.55	63.62	73.79	4.06	0.87	0.24	5.21

Table A3

Proximate and Ultimate Analysis Data for Different Size Fractions of Devco Coal (as received)

Mesh fraction	Proximate analysis				Ultimate analysis				
	Moisture	Ash	Volatile	Fixed carbon (diff.)	C	H	N	S (total)	O (diff.)
	(wt %)				(wt %)				
- 60+100	1.17	2.52	35.04	61.27	85.16	5.23	1.68	0.85	3.39
-100+200	0.89	2.44	35.20	61.47	85.44	5.31	1.73	0.83	3.36
-200+325	0.97	2.50	35.41	61.12	84.34	4.68	1.67	0.85	4.99
-325+400	0.87	2.58	35.14	61.41	84.75	5.22	1.76	0.81	4.01
-400	1.03	2.78	34.60	61.59	85.00	5.23	1.54	0.88	3.54

Table A4

Proximate and Ultimate Analysis Data for Different Size Fractions of Coal No. 3 (as received)

Mesh fraction	Proximate analysis				Ultimate analysis				
	Moisture	Ash	Volatile	Fixed carbon (diff.)	C	H	N	S (total)	O (diff.)
	(wt %)				(wt %)				
- 60+100	5.26	26.66	31.11	36.97	47.31	3.53	0.55	0.34	16.35
-100+200	5.01	26.78	31.25	36.96	45.78	3.55	0.53	0.29	18.06
-200+325	5.03	29.73	30.00	35.24	42.16	3.41	0.49	0.23	18.95
-325+400	5.13	30.31	29.83	34.73	38.85	3.22	0.53	0.29	21.67
-400	3.85	37.24	27.72	31.19	37.33	2.72	0.45	0.23	18.18

Table A5

Analytical Data for -400 Mesh Size Fraction of
Pittsburgh No. 8 and Coal Valley Coals (as received)

Proximate analysis	Coal sample Pittsburgh No. 8	Coal Valley
Moisture (wt %)	2.41	4.57
Ash (wt %)	6.43	16.56
Volatile (wt %)	35.58	23.91
Fixed carbon (wt %) (diff.)	55.58	54.96
Ultimate analysis		
Carbon (C)	76.84	
Hydrogen (H)	5.52	
Nitrogen (N)	1.59	
Oxygen (O)	5.83	
Total sulfur (S)	1.36	
Pyritic sulfur	0.57	
Organic sulfur	0.79	
Sulfatic sulfur	< 0.01	

LEGEND OF FIGURES

Figure 1. Schematic representation of the process of particle adhesion and particle engulfment.

Figure 2. Schematic of the solidification front apparatus.

Figure 3. Photomicrographs of coal particles at the solidification front of thymol illustrating particle size dependence of particle rejection.

Fraction size: 45-74 μm.

Particle diameters: Middle particle = 45 μm;

Right particle = 60 μm;

Left particle = 75 μm.

This sequence of photomicrographs shows the rate of solidification increasing from 5 μm/sec to 8 μm/sec. The right particle is pushed slightly and engulfed. The middle particle is pushed and finally is engulfed as the solidification rate increases. The left particle is engulfed immediately. In each photomicrograph the solidification front is moving diagonally from right to left.

Figure 4. Solidification front velocity, V, as a function of particle diameter, D, for B.C. coal particles in thymol.

Figure 5. Critical velocity, V_c, as a function of particle diameter, D, for three organic matrix materials - coal sample No. 2 (at the melting temperatures of the matrix materials).

Figure 6. Particle surface tension, γ_{pv}, as a function of particle diameter, D, for the three organic matrix materials - coal sample No. 2 (at 20°C).

Figure 7. Contact angle, θ, as a function of particle diameter, D, for the three organic matrix materials - coal sample No. 2 (at 20°C).

Figure 8. Critical velocity, V_c, as a function of particle diameter, D, for coal No. 3 wet and dry screened samples in thymol (at the melting temperature of thymol, at 51.5°C).

Figure 9. Particle surface tension, γ_{PV}, as a function of particle diameter, D, for coal No. 3 wet and dry screened samples in thymol (at the melting temperature of thymol, at 51.5°C).

Figure 10. Solidification front velocity, V, as a function of particle diameter, D, for B.C. coal particles in water/ice.

Figure 11. Particle surface tension, γ_{PV}, as a function of particle diameter, D, for coal No. 3 sample in thymol and in water/ice corrected to 20°C.

Figure 12. The free energy of cohesion, ΔF^{coh}, of Teflon particles as a function of the surface tension of the suspending liquid, γ_{LV}.

Figure 13. Photograph of a sedimentation volume experiment of PTFE powder in mixtures of n-hexane/n-hexadecane. Minimum at $\gamma_{LV} = 20.0$ mJ/m^2.

Figure 14. Sedimentation volume, V_{sed}, as a function of the surface tension, γ_{LV}, of the suspending liquid for polytetrafluoroethylene, PTFE.

Figure 15. Sedimentation volume, V_{sed}, as a function of the surface tension, γ_{LV}, of the suspending liquid for B.C. coal (-400 mesh).

Figure 16. Sedimentation volume, V_{sed}, as a function of the surface tension, γ_{LV}, of the suspending liquid for different size fractions of B.C. coal in n-propanol/ethylene glycol.

Figure 17. Reproducibility of the sedimentation volume measurements in an aqueous medium; results from two separate experiments with Devco coal (-400 mesh) in DMSO/water. Maxima at γ_{LV} = 68.8 and 69.3 mJ/m^2, respectively.

Figure 18. Sedimentation volume, V_{sed}, as a function of the surface tension, γ_{LV}, of the suspending liquid (n-propanol/water) for Pittsburgh coal No. 8. $Maximum_1$ at γ_{LV} = 36.5 mJ/m^2; $maximum_2$ at γ_{LV} = 68.1 mJ/m^2.

Figure 19. The free energy of adhesion, ΔF^{adh}, for particles as a function of substrate surface tension, γ_{SV}: a: $\gamma_{LV} > \gamma_{PV}$;
b: $\gamma_{LV} < \gamma_{PV}$.

Figure 20. Photomicrographs of Devco coal particle adhesion under varying conditions:

(a) Fluorinated ethylene propylene
(FEP): γ_{SV} = 16.4 mJ/m^2 ; γ_{LV} = 72.5 mJ/m^2 ;

(b) Sulfonated polystyrene
(SPS): γ_{SV} = 66.7 mJ/m^2 ; γ_{LV} = 72.5 mJ/m^2 ;

(c) Fluorinated ethylene propylene
(FEP): γ_{SV} = 16.4 mJ/m^2 ; γ_{LV} = 56.1 mJ/m^2 ;

(d) Sulfonated polystyrene
(SPS): γ_{SV} = 66.7 mJ/m^2 ; γ_{LV} = 56.1 mJ/m^2 ;

Suspending liquids are formed from the mixture of various concentrations of n-propanol and water.

Figure 21. Extent of coal particle adhesion (coal No. 3) as a function of substrate surface tension, γ_{SV}, for various n-propanol/water concentrations.

Figure 22. Slopes of the straight lines of Figure 21 as a function of the surface tension, γ_{LV}, of the suspending liquid for coal No. 3. The slope is equal to zero for $\gamma_{LV} = \gamma_{PV}$.

Figure 23. Adhesion of Devco coal particles suspended in a mixture of thiodiethanol/n-propanol (γ_{LV} = 40.0 mJ/m^2) as a function of time. Substrate is polyethyleneterephthalate, γ_{SV} = 47.0 mJ/m^2.

REFERENCES

1. A.M. Gaudin, Flotation, 2nd Ed., McGraw Hill, New York, (1957).
2. R.E. Marganski and R.L. Rowell, J. Disp. Sci. Techn., 4:415 (1983).
3. L. Boruvka and A.W. Neumann, J. Chem. Phys., 66:5464 (1977).
4. L. Boruvka, Y. Rotenberg and A.W. Neumann, Langmuir, 1:40 (1985).
5. H.B. Callen, Thermodynamics, John Wiley & Sons, Inc., New York, 1960.
6. A.W. Neumann and R.J. Good, J. Colloid Interface Sci., 38:341 (1971).
7. A.W. Neumann, R.J. Good, C.J. Hope and M. Sejpal, J. Colloid Interface Sci., 49:291 (1974).
8. C.A. Ward and A.W. Neumann, J. Colloid Interface Sci., 49:286 (1974).
9. O. Driedger, A.W. Neumann and P.J. Sell, Kolloid-Z.u.Z. Polymere, 204:101 (1965).
10. A.W. Neumann, O.S. Hum, D.W. Francis, W.Zingg and C.J. van Oss, J. Biomed. Mater. Res., 14:499 (1980).
11. A.W. Neumann, D.R. Absolom, D.W. Francis and C.J. van Oss, Sep. Purif. Methods., 9:63 (1980).
12. A.F. Taggart, G.R.M. Del Guidice and A.M. Sadler, Trans. AIME, 134:180 (1939).
13. G.A. Brady and A.W. Gauger, Ind. Eng. Chem., 32:1599 (1940).
14. A.W. Neumann and R.J. Good, in Experimental Methods. in Surface and Colloid Science (R.J. Good and R.R. Stromberg, eds.), Vol. 11, Plenum Press, New York, 1979, pp. 31-91.
15. R.M. Horsley and H.G. Smith, Fuel, 30:54 (1951).
16. S.C. Sun, Trans. AIME, 199:67 (1954).
17. T. Murata, Fuel, 60:744 (1981).

18. J. Coca, J.L. Bueno and H. Sastre, Fuel, 61:166 (1982).

19. R.L. Eissler and K.E. van Holde, Illinois State Geological Survey, Circular 333, 1962, pp. 1-20.

20. D.R. Brown, Coal Flotation in Froth Flotation - 50th Anniversary Volume (D.W. Fuerstenau, ed.), Chapter 20, AIME, New York, 1962, pp. 518-538.

21. B.K. Parekh and F.F. Aplan, Rec. Dev. Sep. Sci. (N.N. Li, ed.), Vol. 4, CRC Press, West Palm Beach, Fl., 1978., pp. 107-113.

22. J.A. Gutierrez-Rodrigues, R.J. Purcell Jr. and F.F. Aplan, Colloids and Surfaces, 12:1 (1984).

23. J.A. Gutierrez-Rodrigues and F.F. Aplan, Colloids and Surfaces, 12:27 (1984).

24. E.I. Vargha-Butler, M. Kashi, H.A. Hamza and A.W. Neumann (submitted for publication).

25. M. Kashi, M.A. Sc. Thesis, University of Toronto, Toronto, Canada, 1984.

26. L.F. Brunckhorst, CSIRO, Inst. Energy and Earth Resources, Australia (personal communication).

27. E.I. Vargha-Butler, M.R. Soulard, A.W. Neumann and H.A. Hamza, CIM Bull., 74:54 (1981).

28. A.W. Neumann, Adv. Colloid Interface Sci., 4:105 (1974).

29. Y. Rotenberg, L. Boruvka and A.W. Neumann, J. Colloid Interface Sci., 93:169 (1983).

30. J.K. Spelt, Ph.D. Thesis, University of Toronto, Toronto, Canada, 1985.

31. S.N. Omenyi, R.P. Smith and A.W. Neumann, J. Colloid Interface Sci., 75:117 (1980).

32. S.N. Omenyi, A.W. Neumann and C.J. van Oss, J. Appl. Phys., 52:789 (1981).

33. S.N. Omenyi, A.W. Neumann, W.W. Martin, G.M. Lespinard and R.P. Smith, J. Appl. Phys., 52:796 (1981).

34. A.W. Neumann, S.N. Omenyi and C.J. van Oss, J. Phys. Chem., 86:1267 (1982).

35. R.P. Smith, S.N. Omenyi and A.W. Neumann, in Physicochemical Aspects of Polymer Surfaces (K.L. Mittal, ed.). Vol. 1, Plenum, New York, 1983, pp. 155-171.

36. E.I. Vargha-Butler, T.K. Zubovits, H.A. Hamza and A.W. Neumann, J. Disp. Sci. Techn., 6:357 (1985).

37. A.W. Neumann, D.R. Absolom, W. Zingg and C.J. van Oss, Cell Biophys., 1:79 (1979).

38. D.R. Absolom, W. Zingg, C. Thomson, Z. Policova, C.J. van Oss and A.W. Neumann, J. Colloid Interface Sci., 104:51 (1985).

39. R.P. Smith, D.R. Absolom, J.K. Spelt and A.W. Neumann, J. Colloid Interface Sci. (accepted for publication).

40. S.N. Omenyi and A.W. Neumann,, J. Appl. Phys., 47:3956 (1976).

41. M.R. Soulard, E.I. Vargha-Butler, H.A. Hamza and A.W. Neumann, Chem. Eng. Commun., 21:329 (1983).

42. A.W. Neumann, Z. physik Chem. Neue Folge, 41:339 (1964).

43. E.I. Vargha-Butler, T.K. Zubovits, R.P. Smith, I.H.L. Tsim, H.A. Hamza and A.W. Neumann, Colloids and Surfaces, 8:231 (1984).

44. A.W. Neumann, E.I. Vargha-Butler, H.A. Hamza and D.R. Absolom, Colloids and Surfaces (accepted for publication).

45. A.W. Neumann, J.K. Spelt, R.P. Smith, D.W. Francis, Y. Rotenberg and D.R. Absolom, J. Colloid Interface Sci., 102:278 (1984).

46. E.I. Vargha-Butler, E. Moy and A.W. Neumann, 5th International Conference on Surface and Colloid Science, Potsdam, N.Y., 1985, Paper No. 110.

47. E.I. Vargha-Butler, T.K. Zubovits, D.R. Absolom, A.W. Neumann and H.A. Hamza, Chem. Eng. Commun., 33:255 (1985).

48. E.I. Vargha-Butler, T.K. Zubovits, M.K. Weibel, D.R. Absolom and A.W. Neumann, Colloids and Surfaces, 15:233 (1985).

49. D.R. Absolom, K. Eom, E.I. Vargha-Butler and A.W. Neumann, Colloids and Surfaces (accepted for publication).

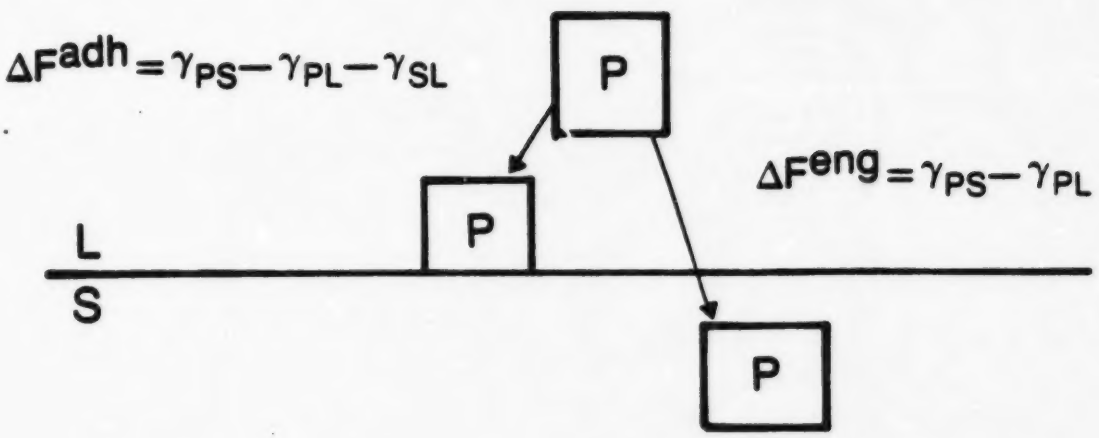
$\Delta F^{adh} = \gamma_{PS} - \gamma_{PL} - \gamma_{SL}$
P
$\Delta F^{eng} = \gamma_{PS} - \gamma_{PL}$
P
L
S
P

Figure 1

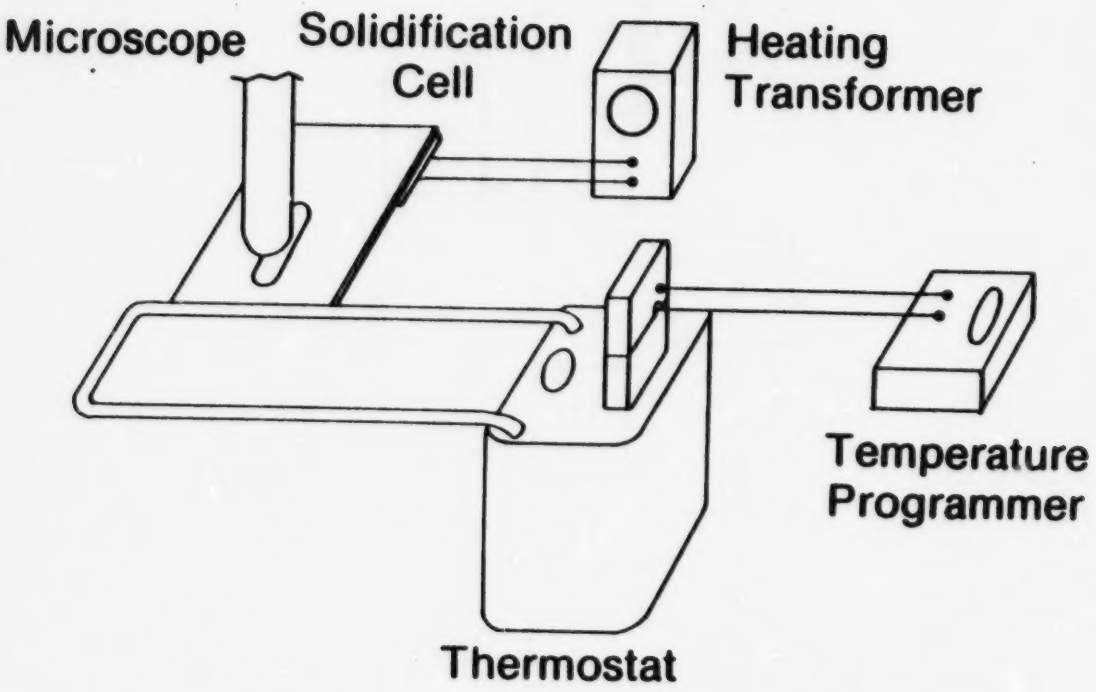
Microscope
Solidification Cell
Heating Transformer
Temperature Programmer
Thermostat

Figure 2

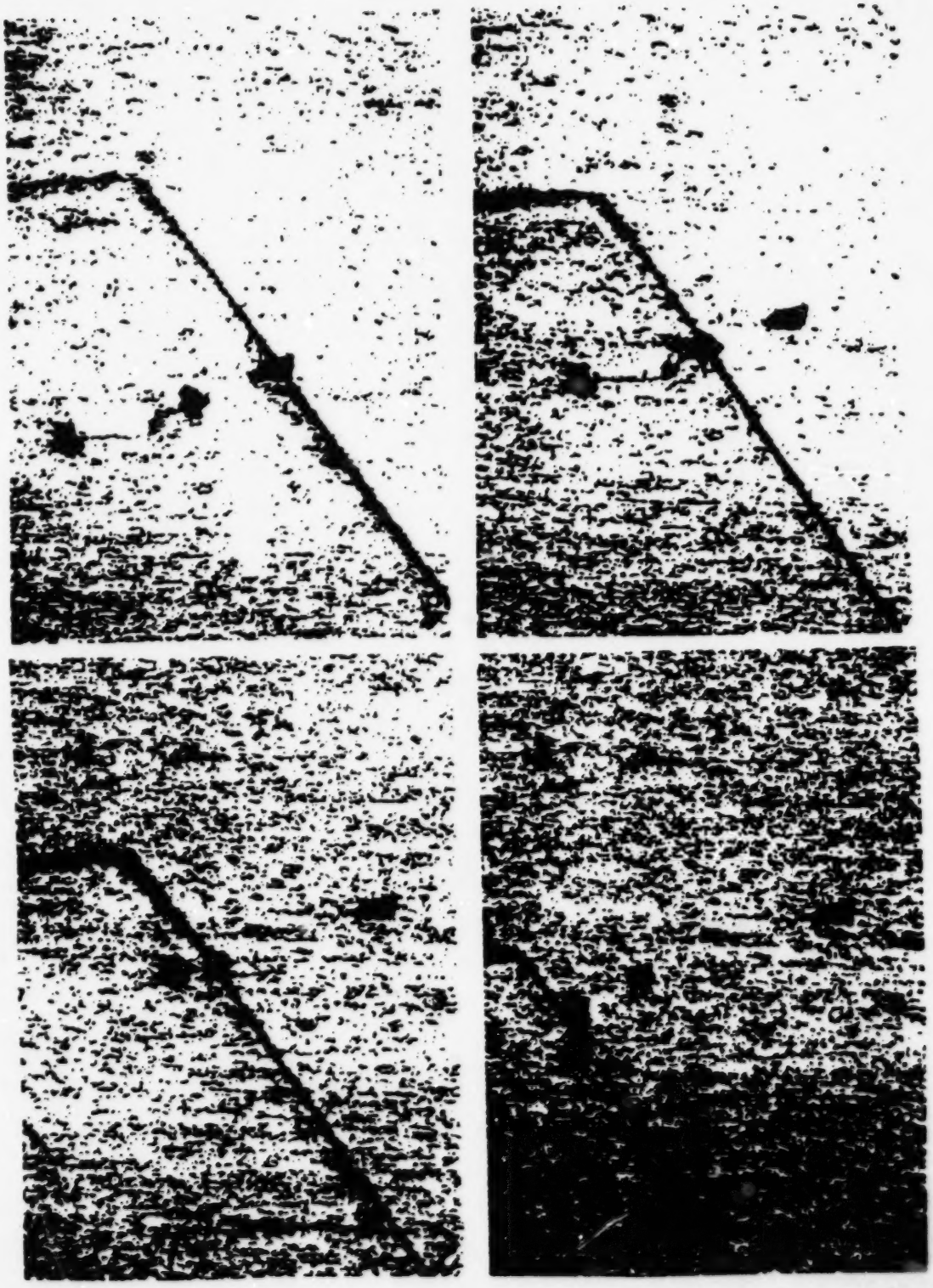

Figure 3

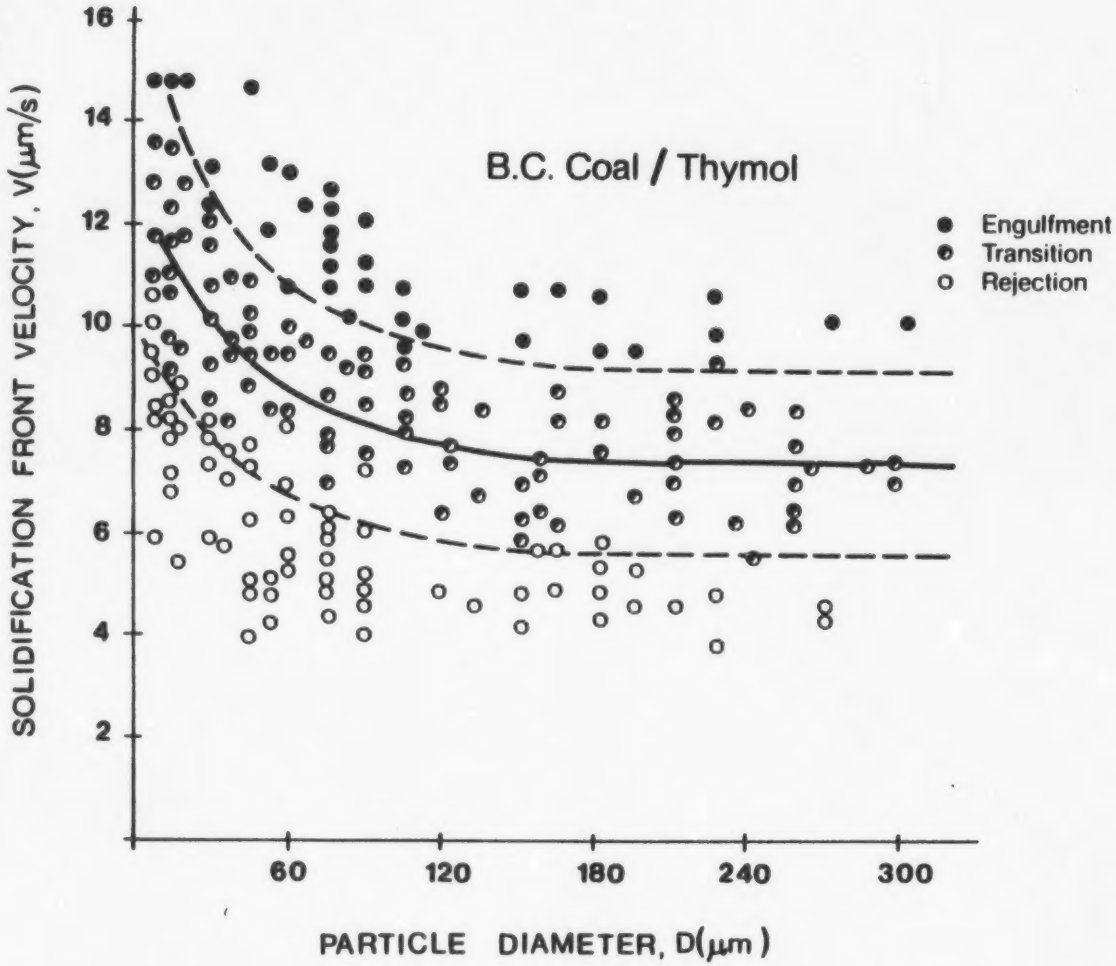
B.C. Coal / Thymol
Engulfment
Transition
Rejection
SOLIDIFICATION FRONT VELOCITY, V(μm/s)
PARTICLE DIAMETER, D(μm)
16
14
12
10
8
6
4
2
60
120
180
240
300

Figure 4

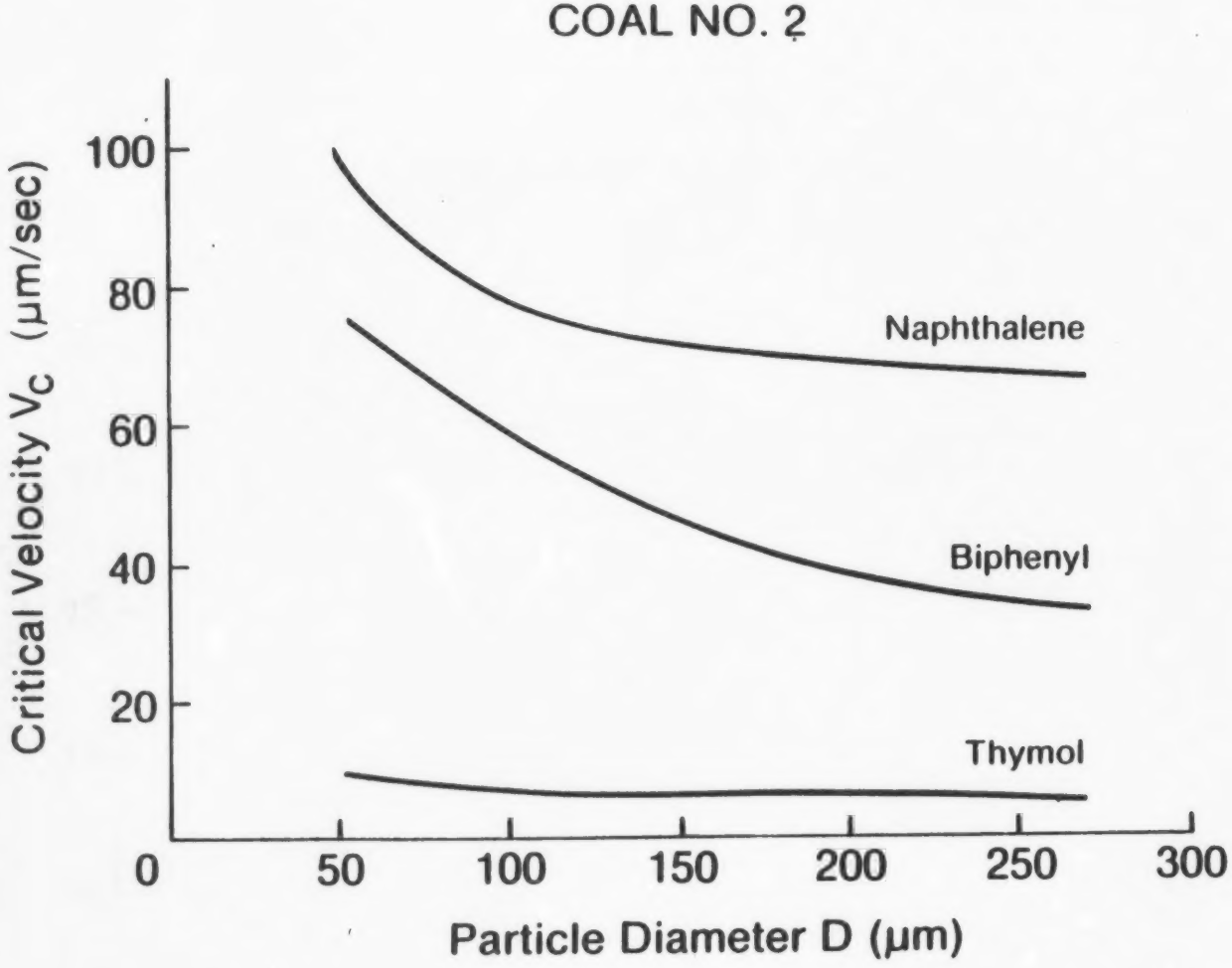
COAL NO. 2
Critical Velocity V_c (μm/sec)
100
80
60
40
20
0
50
100
150
200
250
300
Particle Diameter D (μm)
Naphthalene
Biphenyl
Thymol

Figure 5

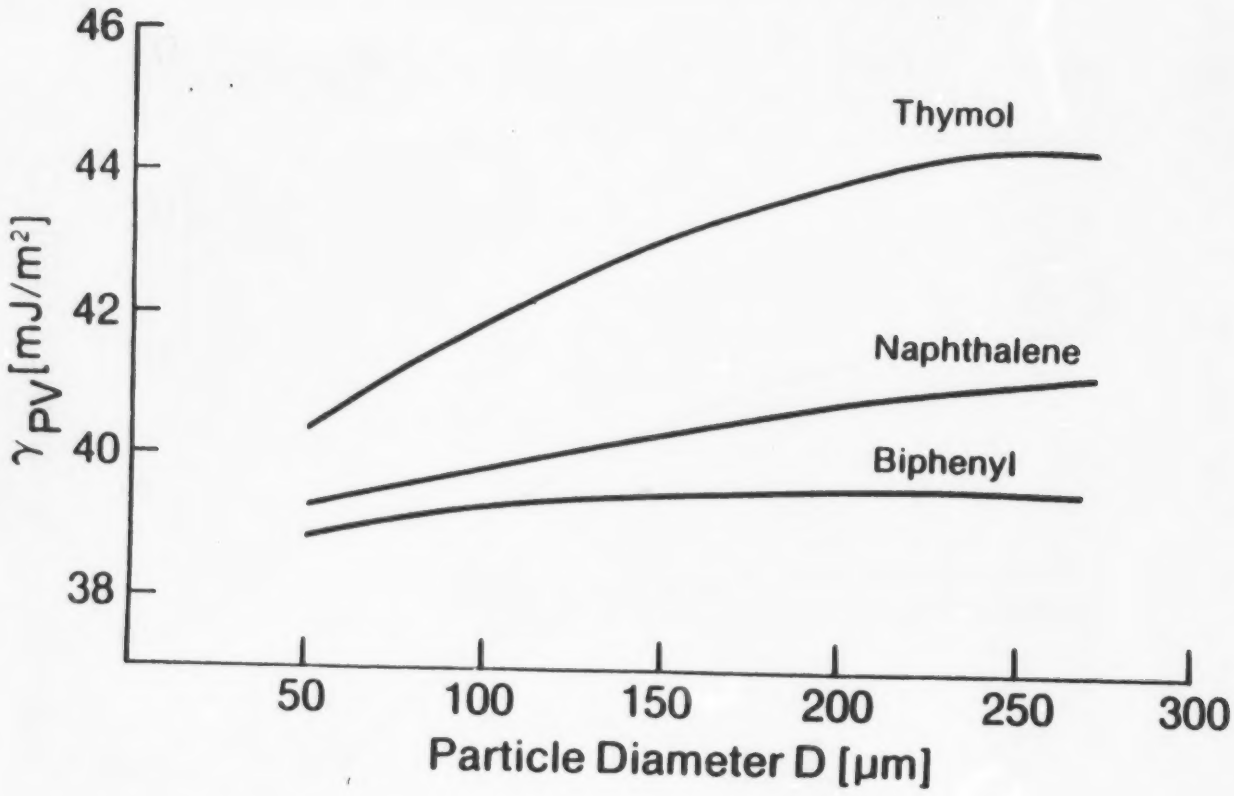
46
44
42
40
38
γ_{PV}[mJ/m²]
Thymol
Naphthalene
Biphenyl
50
100
150
200
250
300
Particle Diameter D [µm]

Figure 6

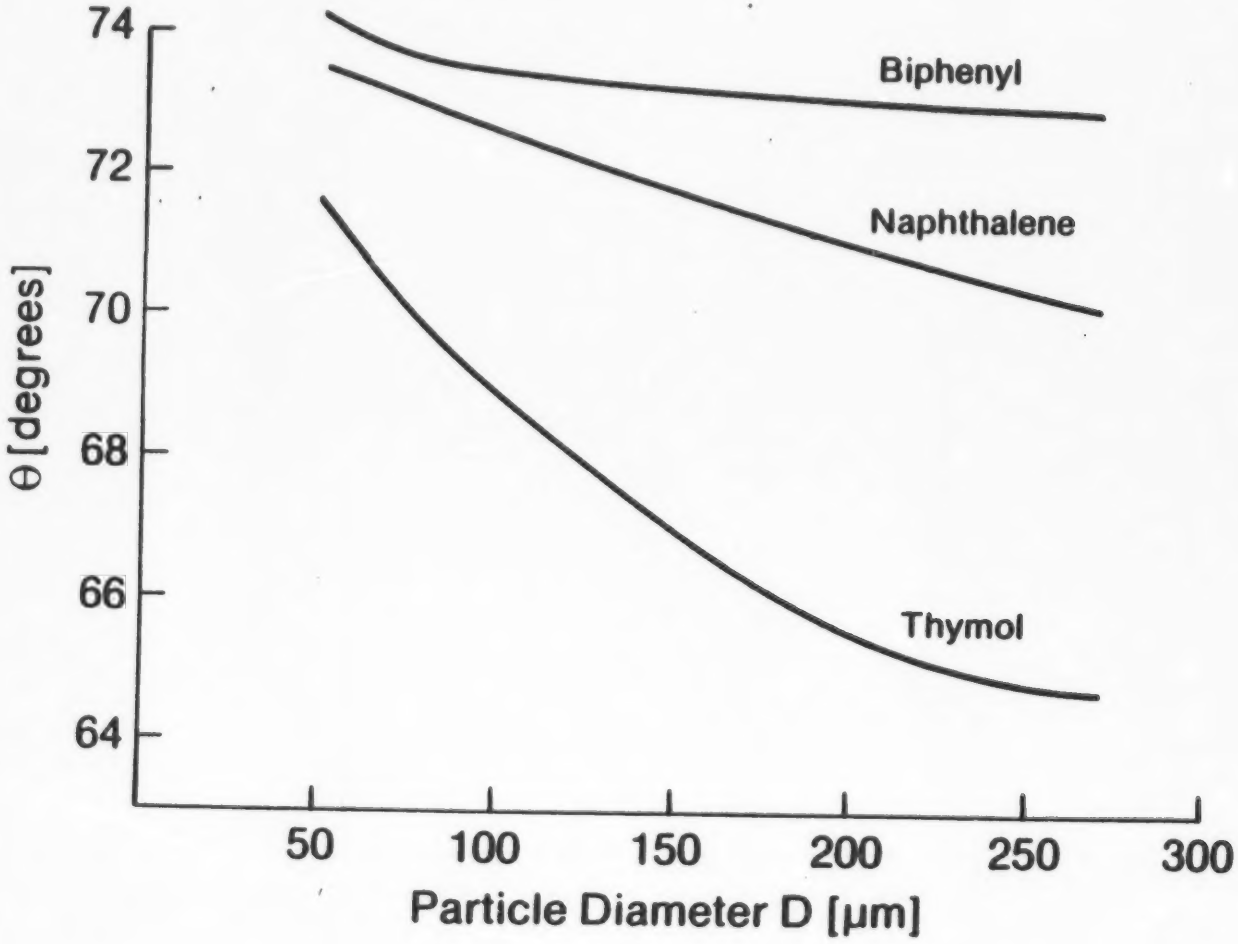
74
72
70
68
66
64
Θ [degrees]
Biphenyl
Naphthalene
Thymol
50
100
150
200
250
300
Particle Diameter D [μm]

Figure 7

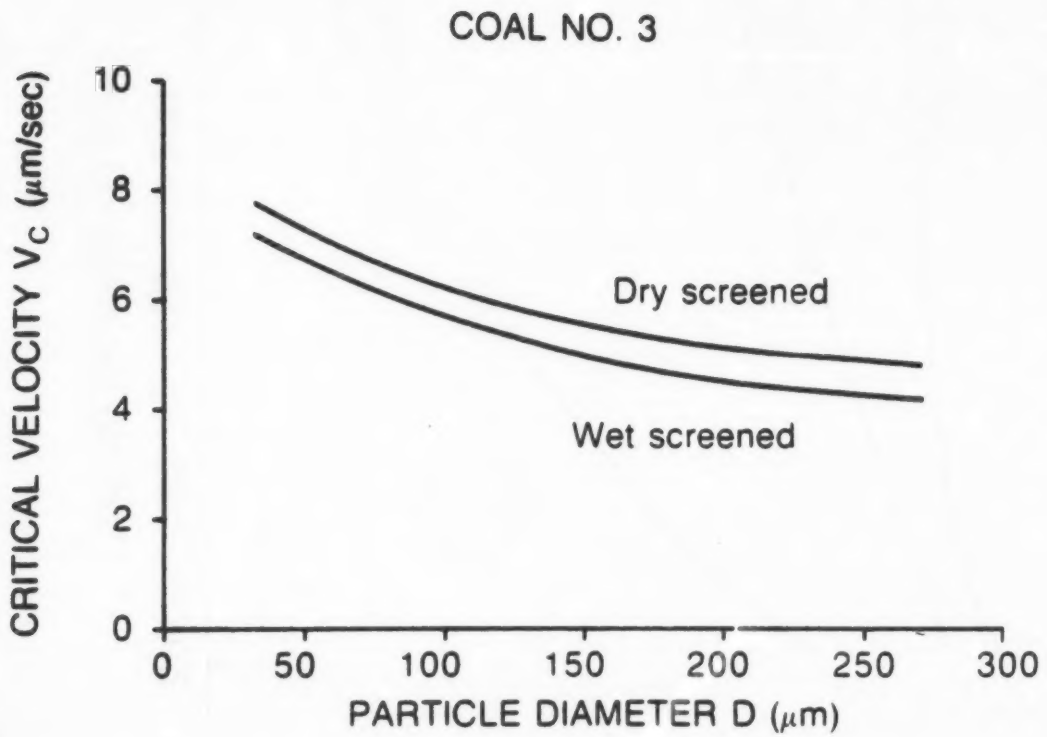
COAL NO. 3
CRITICAL VELOCITY V_C (μm/sec)
10
8
6
4
2
0
Dry screened
Wet screened
0
50
100
150
200
250
300
PARTICLE DIAMETER D (μm)

Figure 8

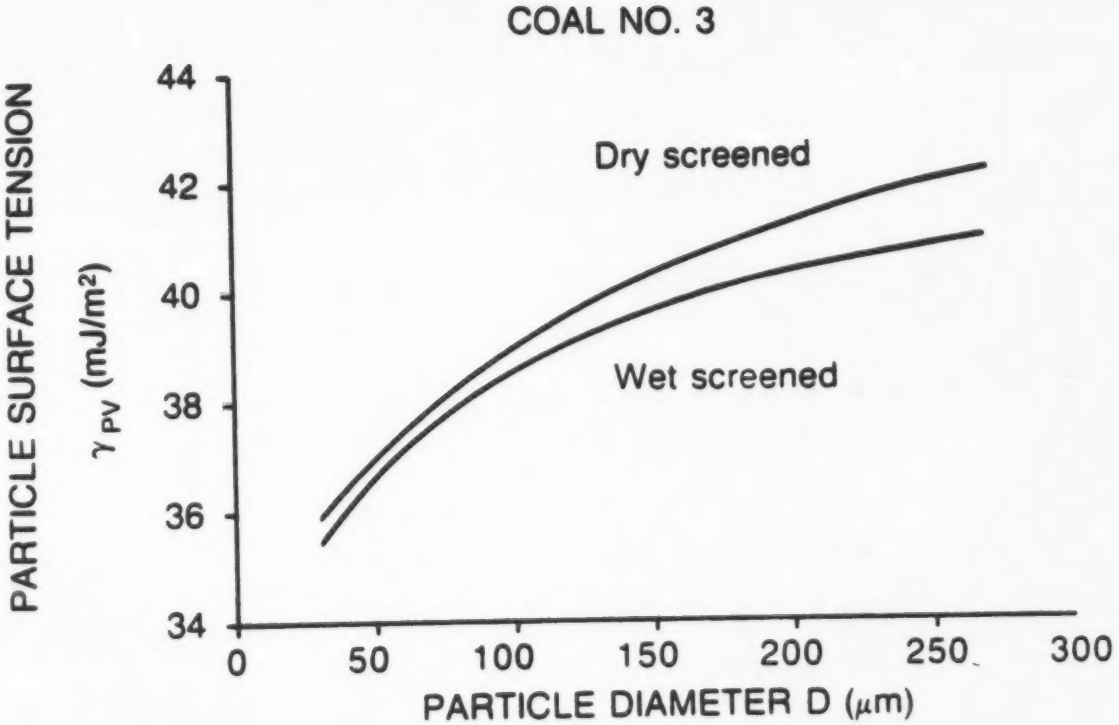
COAL NO. 3
PARTICLE SURFACE TENSION
γ_{PV} (mJ/m²)
44
42
40
38
36
34
Dry screened
Wet screened
0
50
100
150
200
250
300
PARTICLE DIAMETER D (μm)

Figure 9

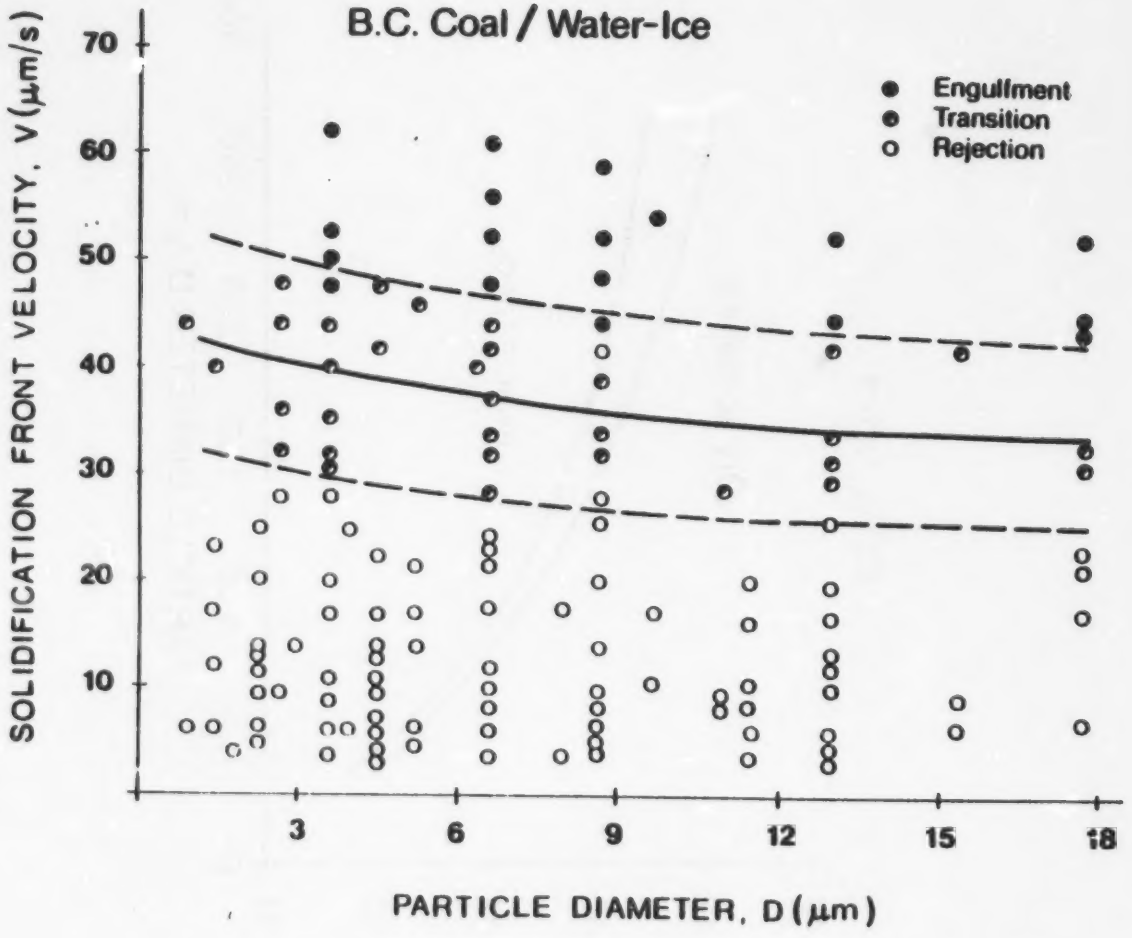
B.C. Coal / Water-Ice
Engulfment
Transition
Rejection
SOLIDIFICATION FRONT VELOCITY, V (μm/s)
70
60
50
40
30
20
10
3
6
9
12
15
18
PARTICLE DIAMETER, D (μm)

Figure 10

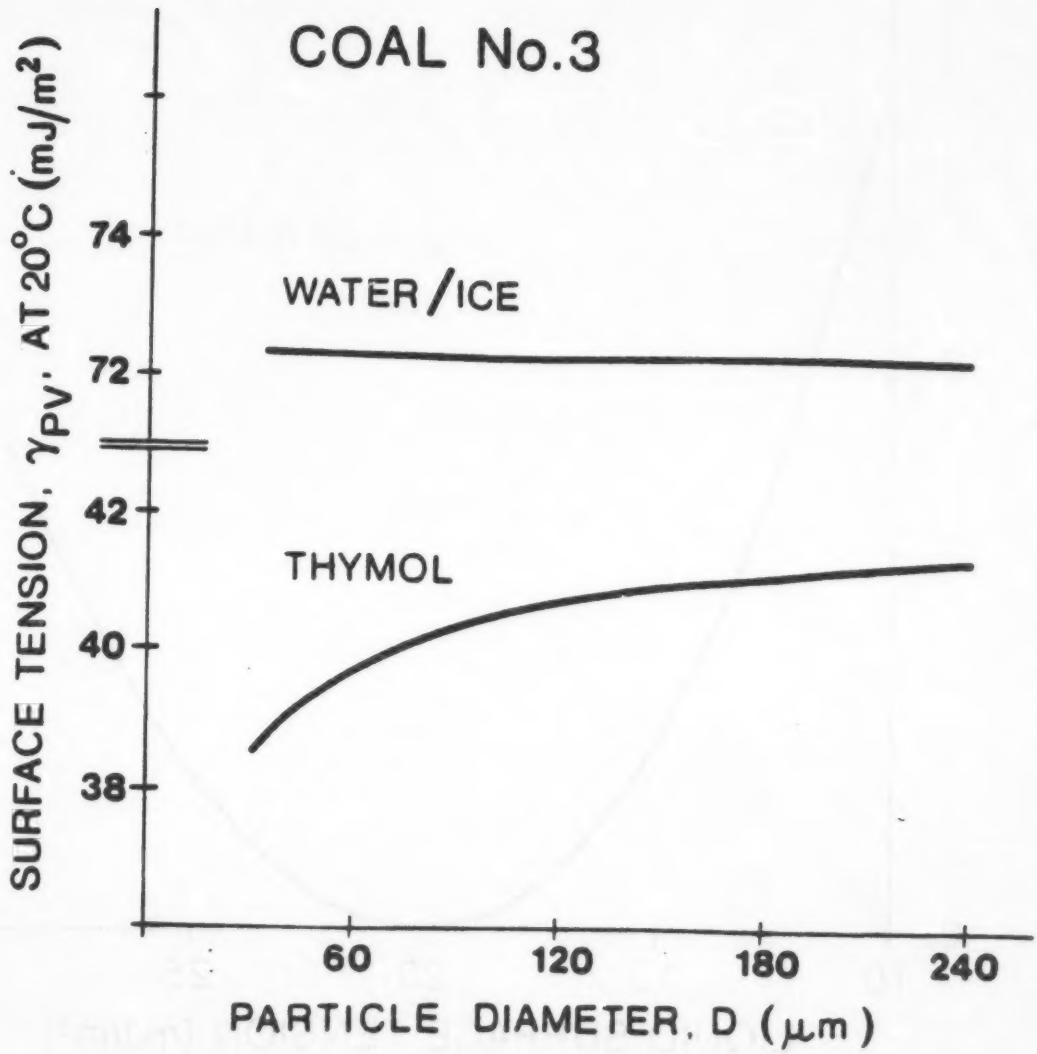
COAL No.3
SURFACE TENSION, γ_{PV}, AT 20°C (mJ/m²)
74
72
42
40
38
WATER/ICE
THYMOL
60
120
180
240
PARTICLE DIAMETER, D (μm)

Figure 11

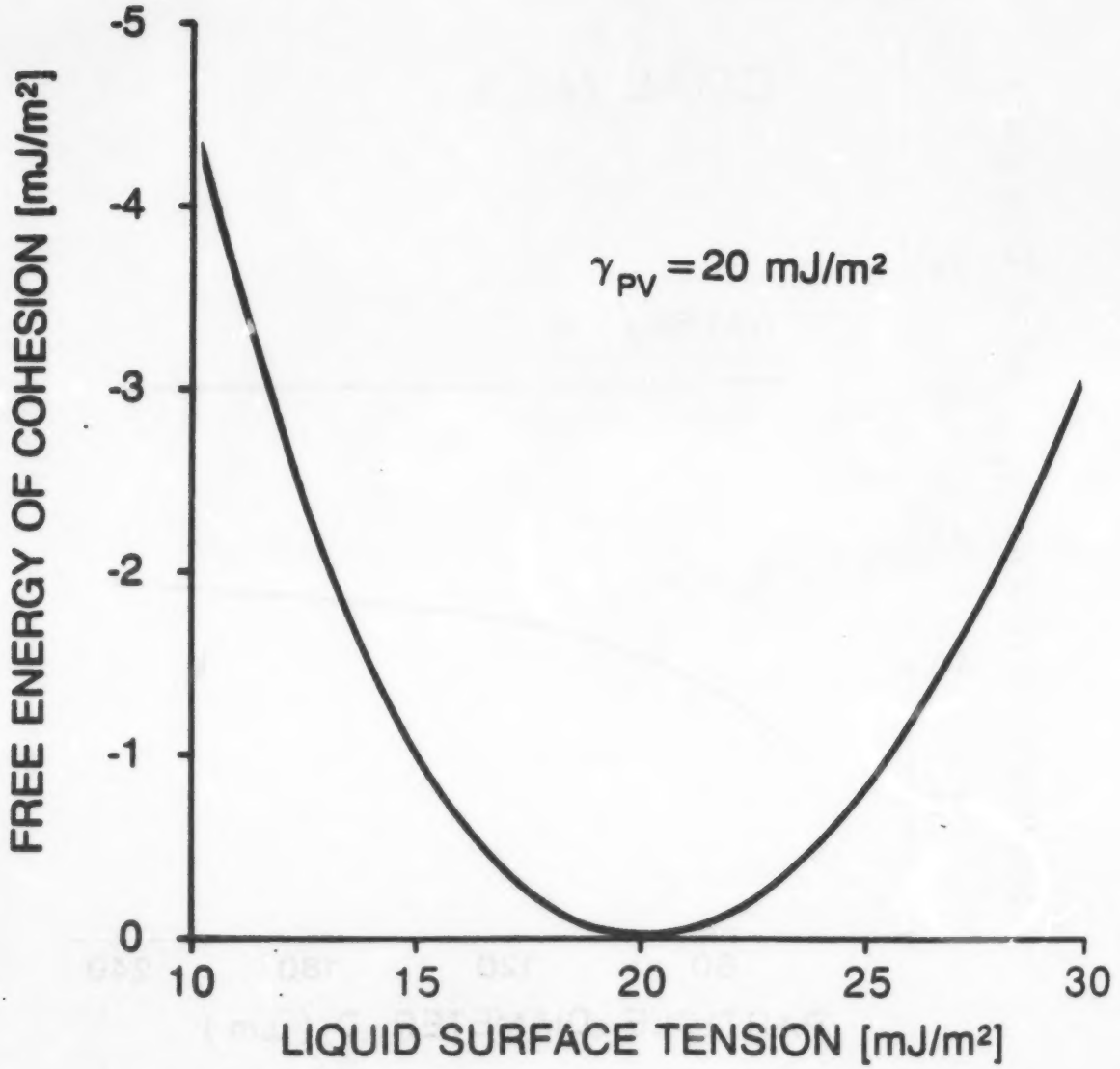
FREE ENERGY OF COHESION [mJ/m²]
-5
-4
-3
-2
-1
0
10
15
20
25
30
LIQUID SURFACE TENSION [mJ/m²]
$\gamma_{PV} = 20$ mJ/m²

Figure 12

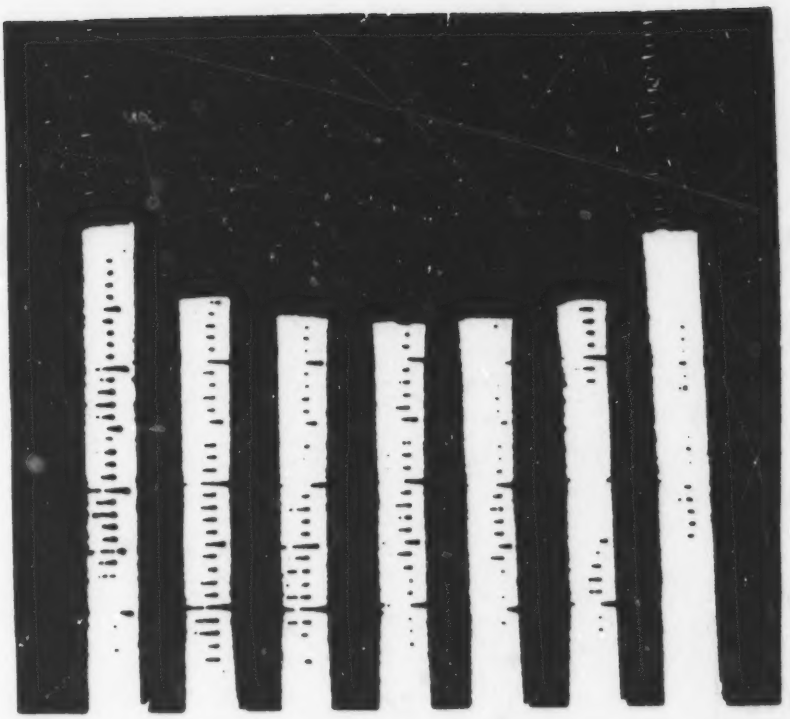

Figure 13

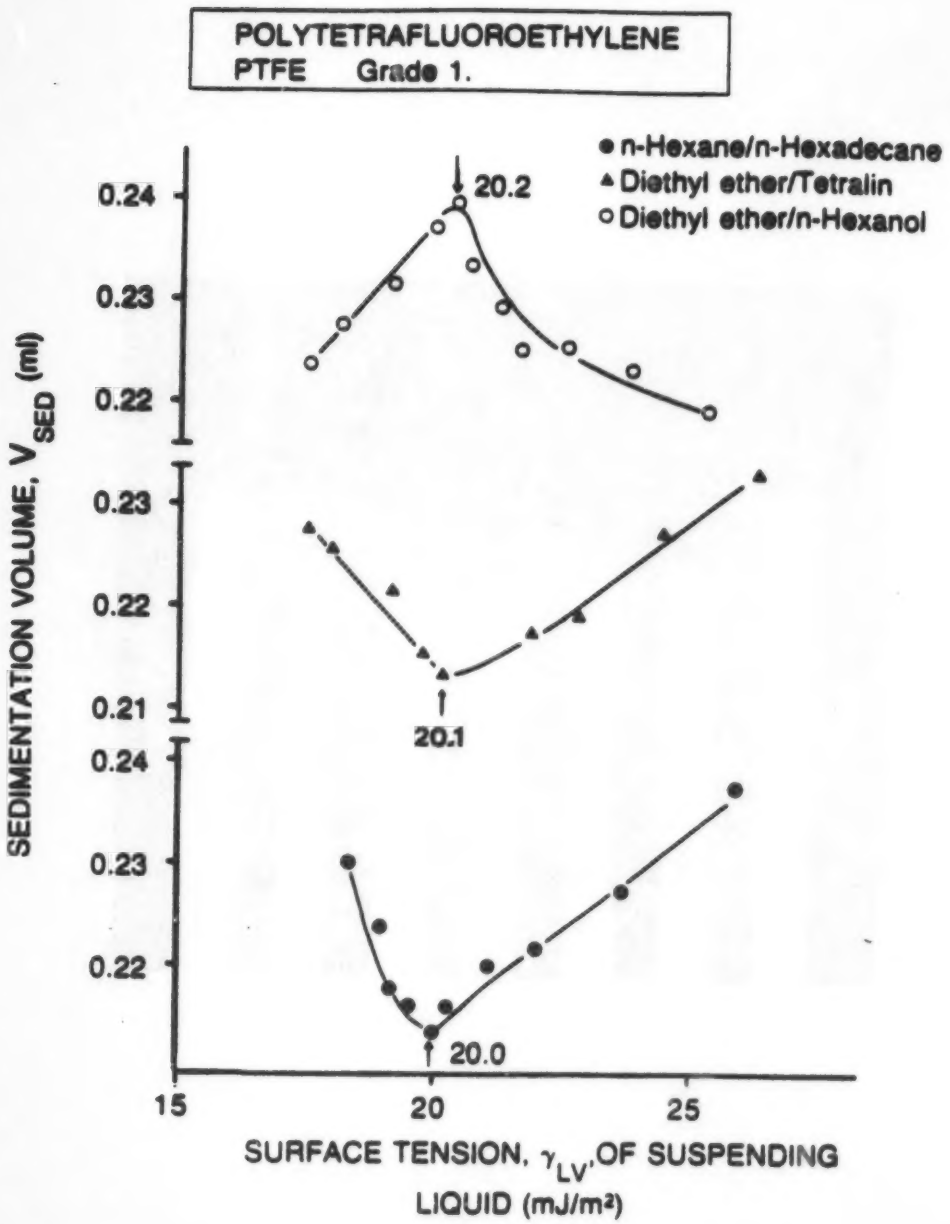
POLYTETRAFLUOROETHYLENE
PTFE Grade 1.
n-Hexane/n-Hexadecane
Diethyl ether/Tetralin
Diethyl ether/n-Hexanol
20.2
20.1
20.0
0.24
0.23
0.22
0.23
0.22
0.21
0.24
0.23
0.22
SEDIMENTATION VOLUME, V_{SED} (ml)
15
20
25
SURFACE TENSION, γ_{LV}, OF SUSPENDING LIQUID (mJ/m²)

Figure 14

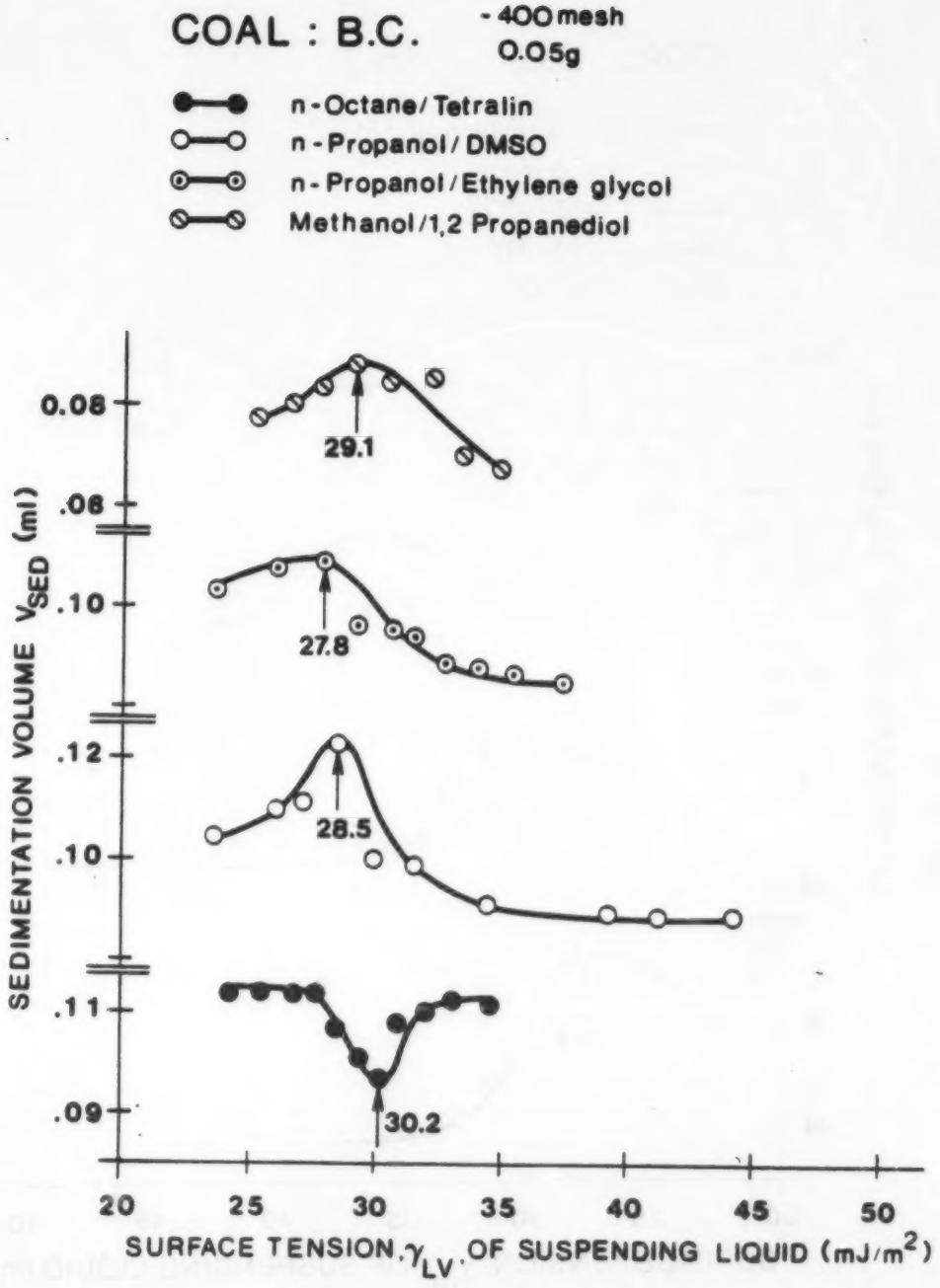
COAL : B.C.
-400 mesh
0.05g
n-Octane/Tetralin
n-Propanol/DMSO
n-Propanol/Ethylene glycol
Methanol/1,2 Propanediol
SEDIMENTATION VOLUME V_{SED} (ml)
0.08
.08
.10
.12
.10
.11
.09
29.1
27.8
28.5
30.2
20
25
30
35
40
45
50
SURFACE TENSION, γ_{LV}, OF SUSPENDING LIQUID (mJ/m^2)

Figure 15

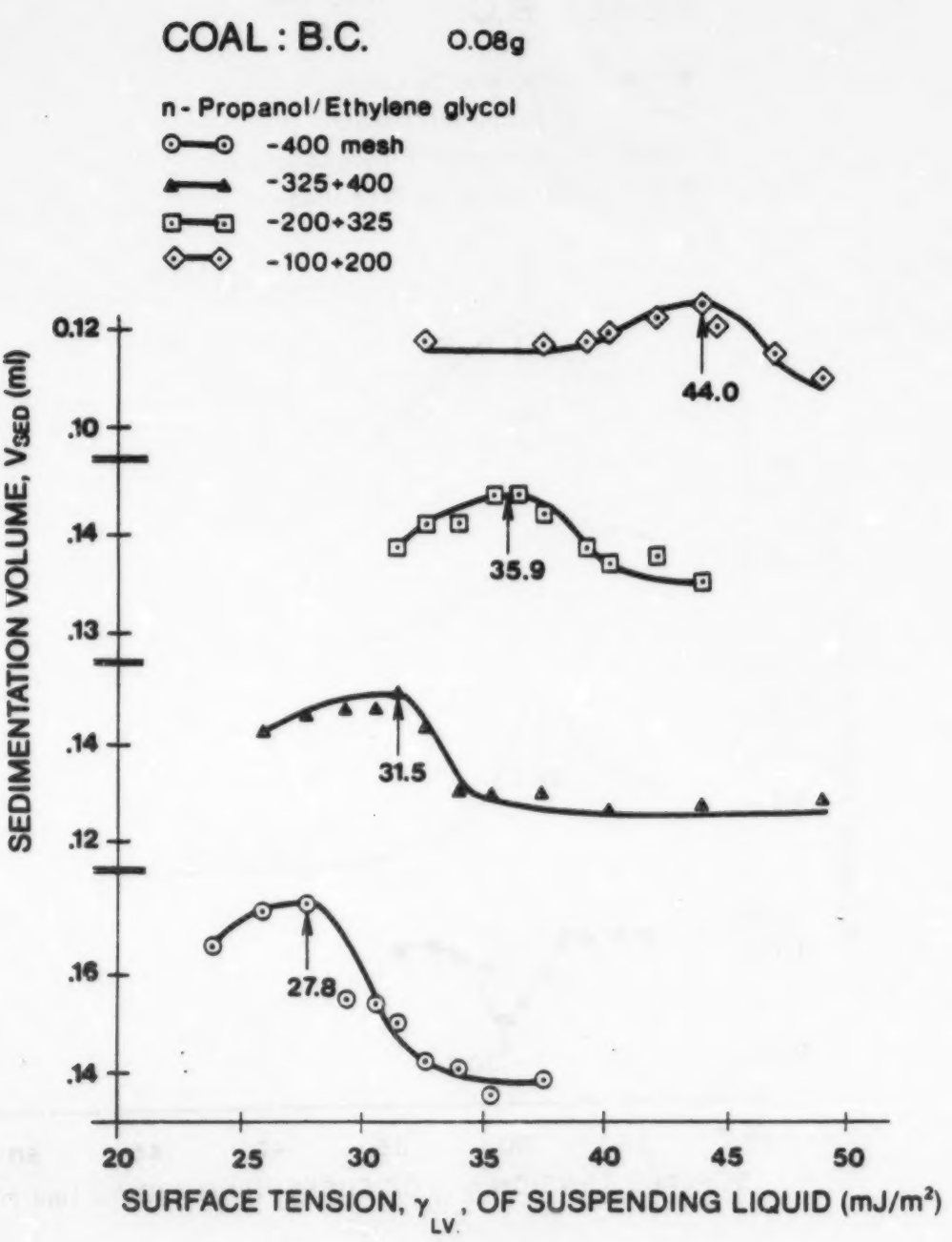
COAL : B.C. 0.08g
n - Propanol / Ethylene glycol
-400 mesh
-325+400
-200+325
-100+200
44.0
35.9
31.5
27.8
SEDIMENTATION VOLUME, V_{SED} (ml)
0.12
.10
.14
.13
.14
.12
.16
.14
20
25
30
35
40
45
50
SURFACE TENSION, γ_{LV}, OF SUSPENDING LIQUID (mJ/m²)

Figure 16

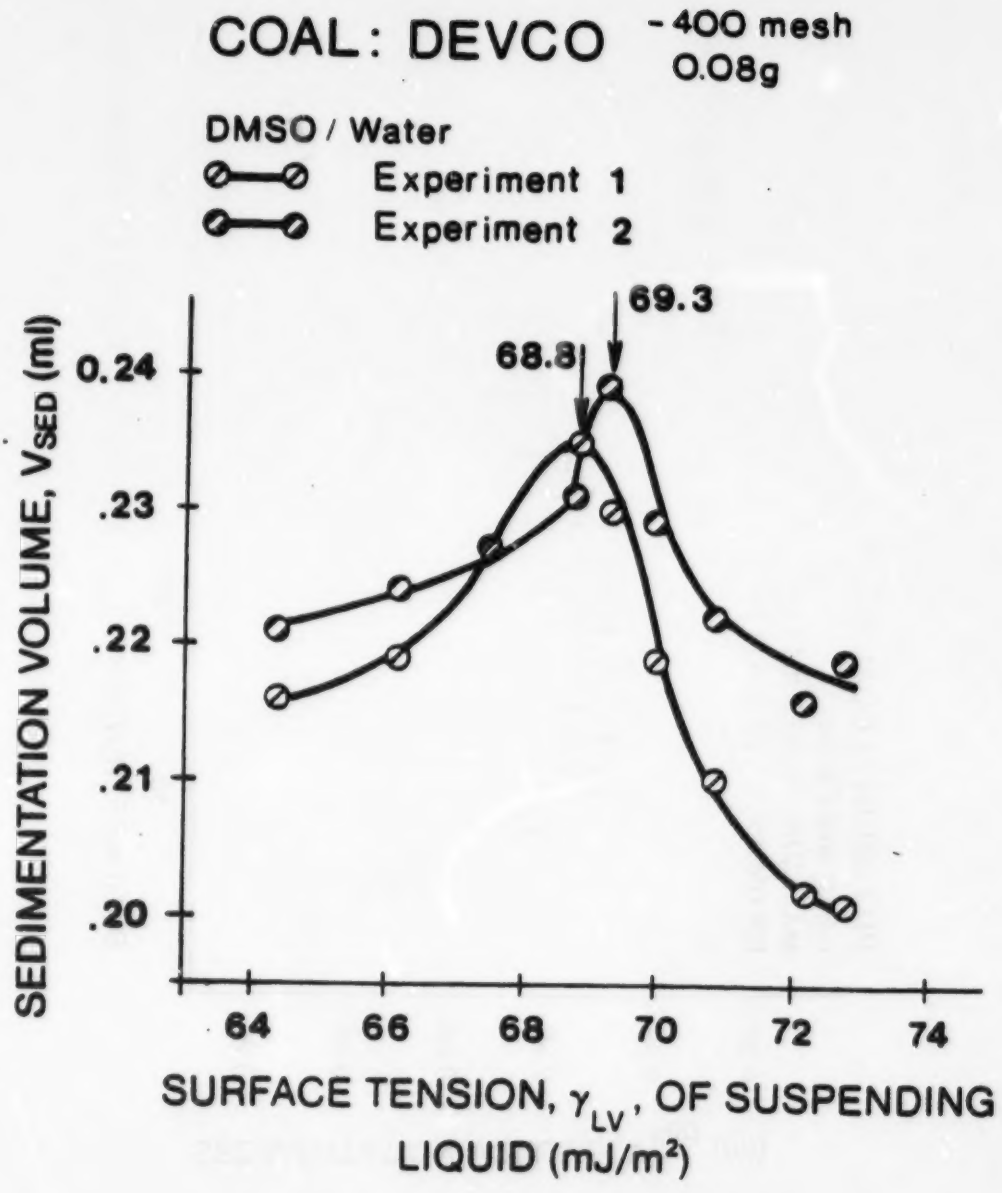
COAL: DEVCO
-400 mesh
0.08g
DMSO / Water
Experiment 1
Experiment 2
69.3
68.8
0.24
.23
.22
.21
.20
SEDIMENTATION VOLUME, V_{SED} (ml)
64
66
68
70
72
74
SURFACE TENSION, γ_{LV}, OF SUSPENDING LIQUID (mJ/m²)

Figure 17

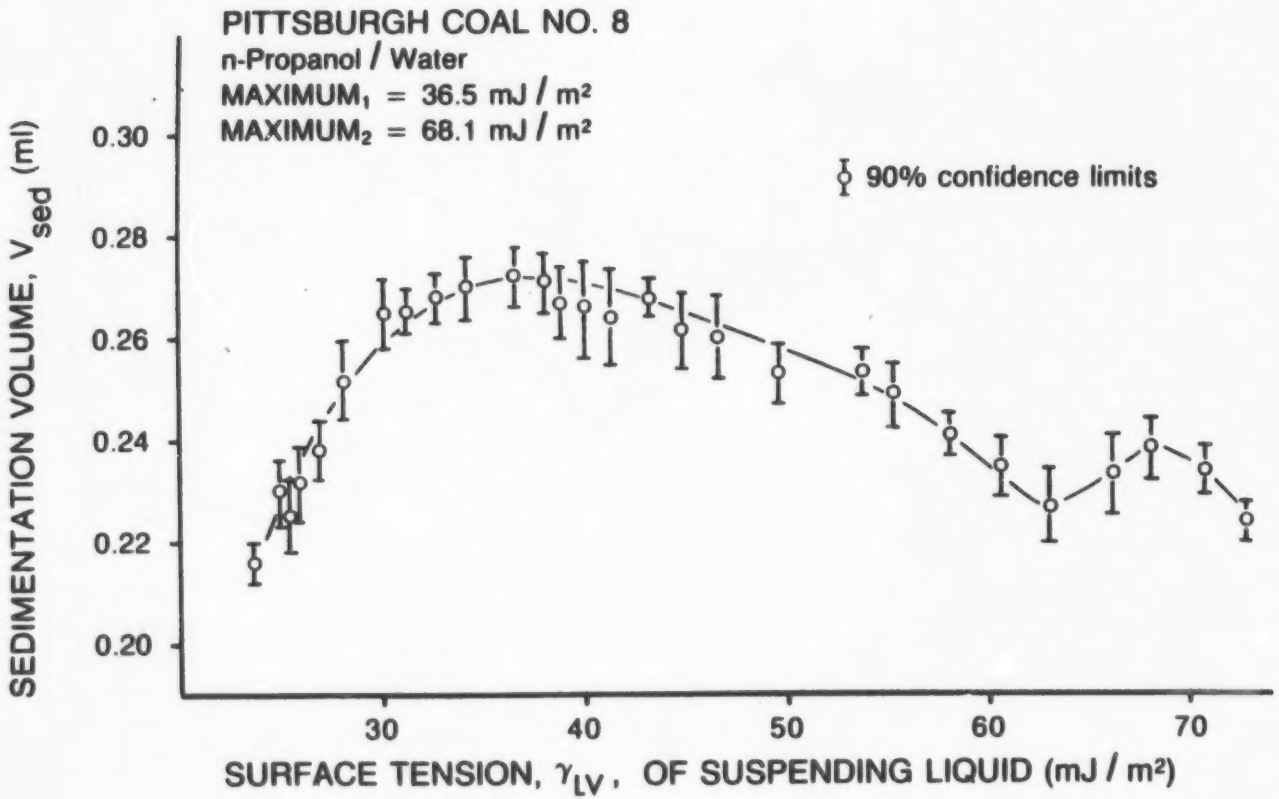
PITTSBURGH COAL NO. 8
n-Propanol / Water
MAXIMUM1 = 36.5 mJ / m2
MAXIMUM2 = 68.1 mJ / m2
90% confidence limits
SEDIMENTATION VOLUME, Vsed (ml)
0.30
0.28
0.26
0.24
0.22
0.20
30
40
50
60
70
SURFACE TENSION, γLV, OF SUSPENDING LIQUID (mJ / m2)

Figure 18

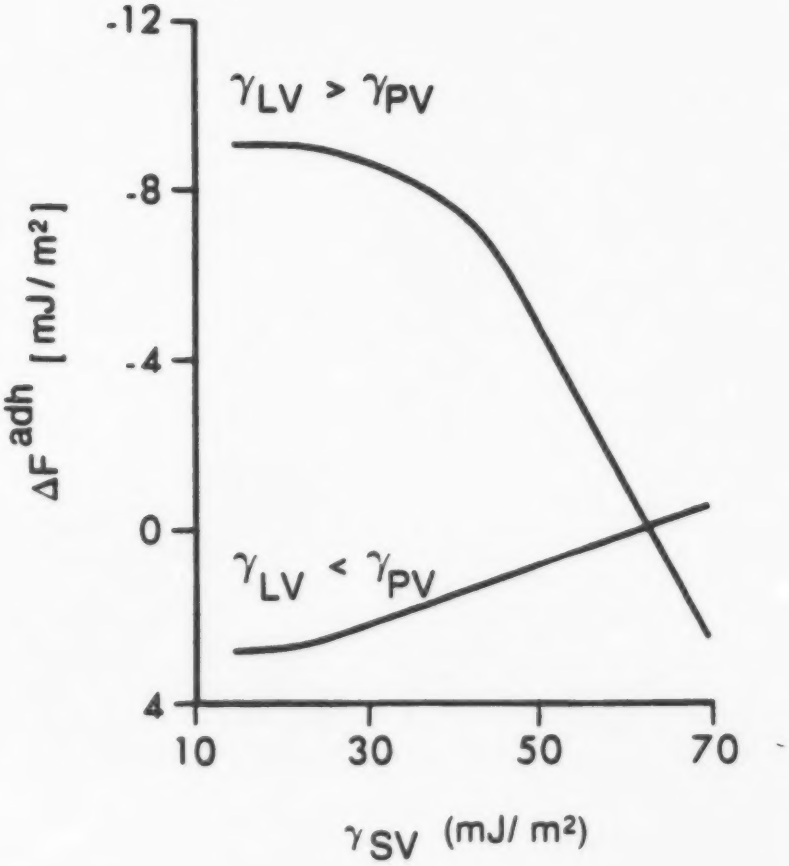
-12
-8
-4
0
4
10
30
50
70
$\gamma_{LV} > \gamma_{PV}$
$\gamma_{LV} < \gamma_{PV}$
ΔF^{adh} [mJ/m²]
γ_{SV} (mJ/m²)

Figure 19

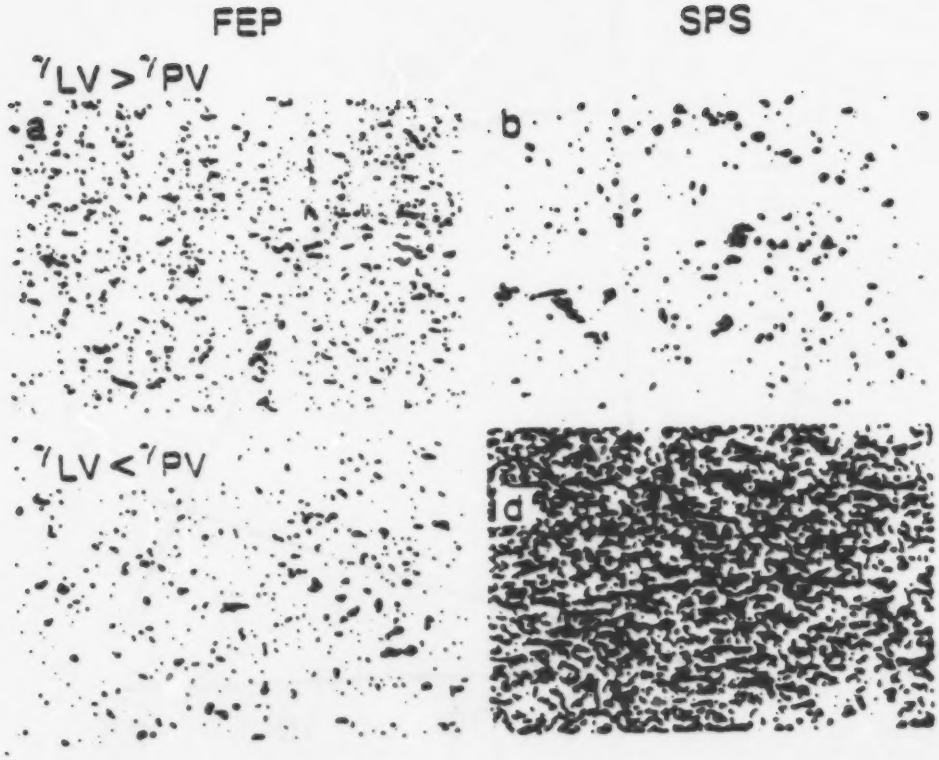

Figure 20

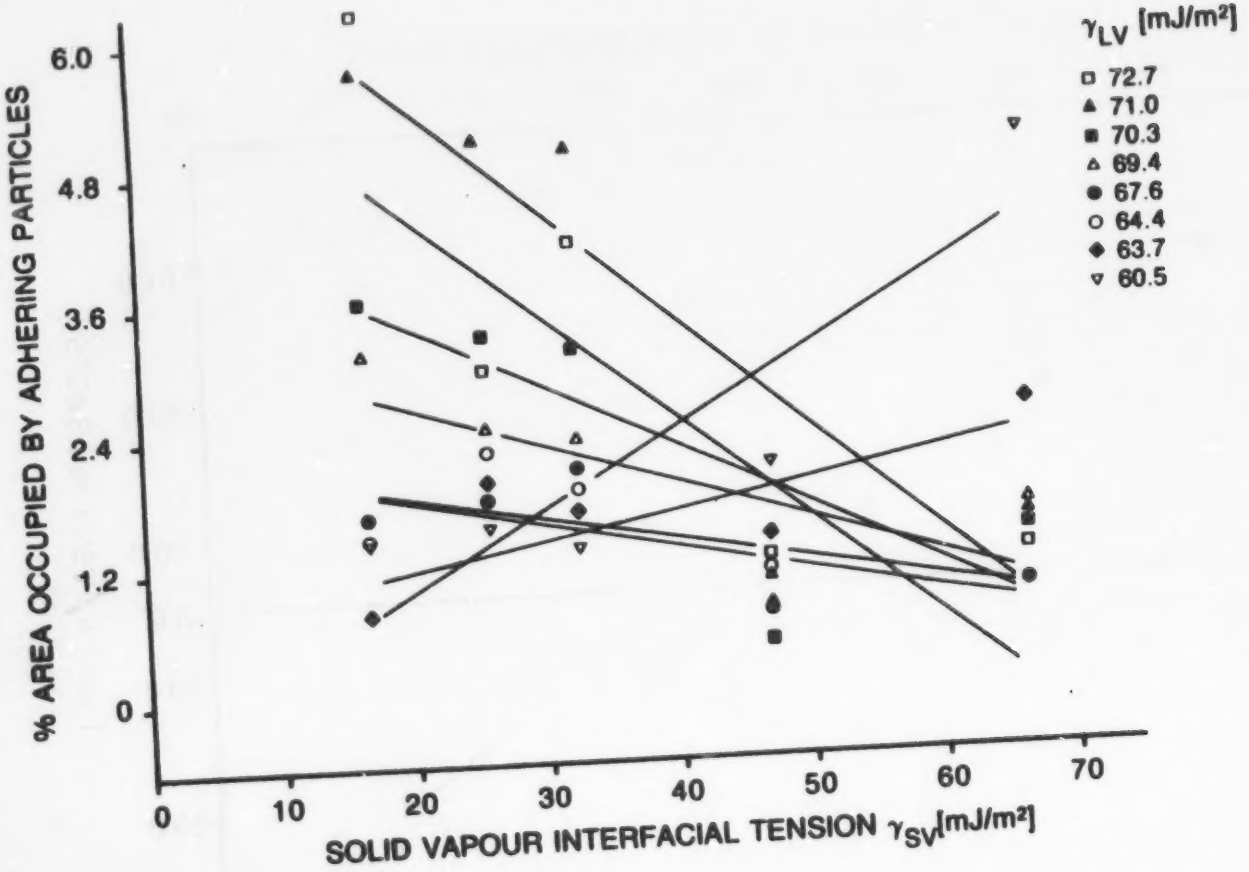
% AREA OCCUPIED BY ADHERING PARTICLES
6.0
4.8
3.6
2.4
1.2
0
0
10
20
30
40
50
60
70
SOLID VAPOUR INTERFACIAL TENSION γ_{SV}[mJ/m²]
γ_{LV} [mJ/m²]
72.7
71.0
70.3
69.4
67.6
64.4
63.7
60.5

Figure 21

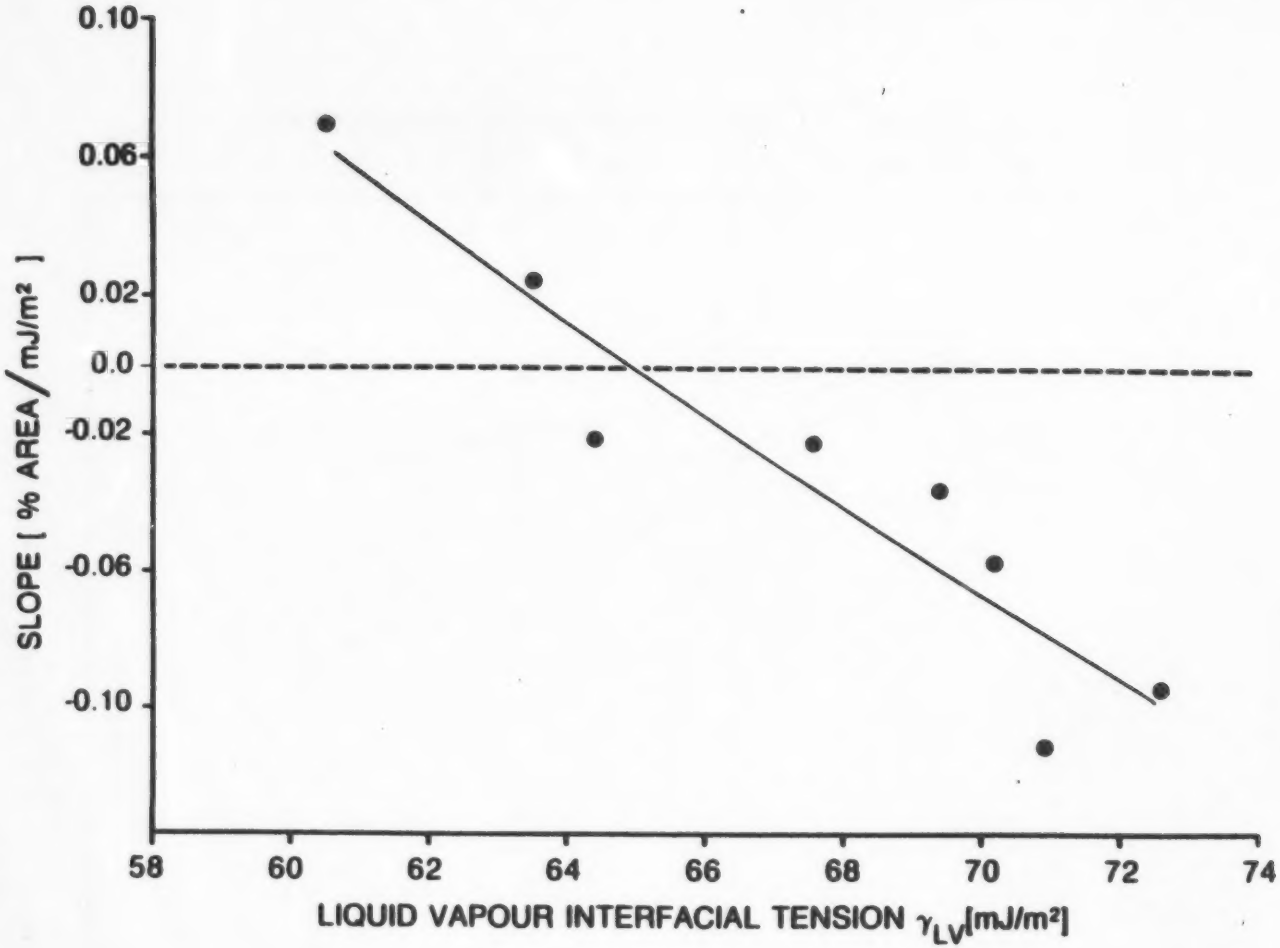
0.10
0.06
0.02
0.0
-0.02
-0.06
-0.10
SLOPE [% AREA / mJ/m²]
58
60
62
64
66
68
70
72
74
LIQUID VAPOUR INTERFACIAL TENSION γ_{LV}[mJ/m²]

Figure 22

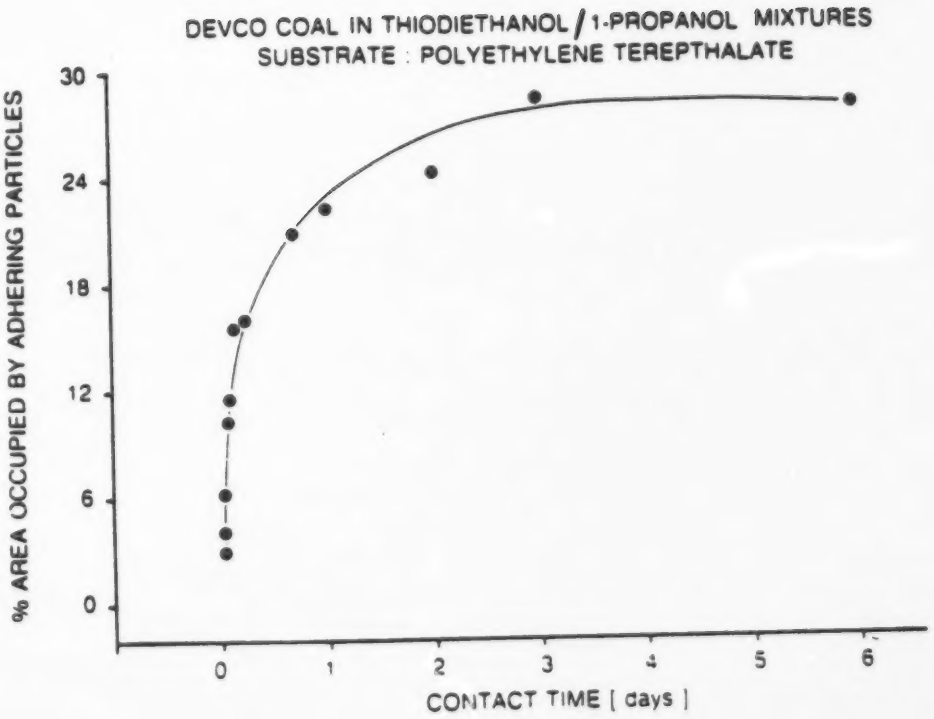
DEVCO COAL IN THIODIETHANOL / 1-PROPANOL MIXTURES
SUBSTRATE : POLYETHYLENE TEREPTHALATE
% AREA OCCUPIED BY ADHERING PARTICLES
30
24
18
12
6
0
0
1
2
3
4
5
6
CONTACT TIME [days]

Figure 23